UNIVERSIDADE FEDERAL DO RIO GRANDE DO SUL

INSTITUTO DE CIÊNCIAS BÁSICAS DA SAÚDE

PROGRAMA DE PÓS-GRADUAÇÃO EM CIÊNCIAS BIOLÓGICAS:

BIOQUÍMICA

Pedro Ozorio Brum

INFLAMAÇÃO HIPOCAMPAL LEVA A ALTERAÇÕES NO SONO REM EM UM MODELO DE NEURODEGENERAÇÃO INDUZIDA POR LPS SISTÊMICO

Porto Alegre, 2021

Pedro Ozorio Brum

INFLAMAÇÃO HIPOCAMPAL LEVA A ALTERAÇÕES NO SONO REM EM UM MODELO DE NEURODEGENERAÇÃO INDUZIDA POR LPS SISTÊMICO

Dissertação apresentada ao Programa de Pós-Graduação em Ciências Biológicas: Bioquímica do Instituto de Ciências Básicas da Saúde da Universidade Federal do Rio Grande do Sul como requisito parcial para a obtenção do título de mestre em Bioquímica.

Orientador: Prof. Dr. Daniel Pens Gelain

Co-Orientadora: Profª. Drª. Maria Elisa Calcagnotto

Porto Alegre, 2021

Agradecimentos

Gostaria de agradecer a Universidade Federal do Rio Grande do Sul, ao Departamento de Bioquímica, ao Programa de Pós-Graduação em Ciências Biológicas - Bioquímica e aos órgãos de fomento: CNPq, CAPES, PROPESQ-UFRGS e FAPERGS por tornarem possível a realização do meu trabalho de mestrado. Ao Centro de Estudos em Estresse Oxidativo, lugar que me acolheu desde o começo da minha trajetória acadêmica, em especial aos professores José Cláudio e Daniel, fica o meu mais sincero agradecimento por todo aprendizado e suporte durante os seis anos em que tive o prazer de trabalhar no laboratório 32.

Professor Daniel, sou extremamente grato por todo o crescimento como cientista que obtive sob tua orientação. Em todos esses anos, tu me ajudou a criar a fundação da minha vida acadêmica. Obrigado pela disponibilidade e apoio como orientador, mas também como amigo. Obrigado por ter me recebido no laboratório 32, onde conheci grandes amigos e cientistas. Todas as pessoas incríveis que passaram por esse laboratório nos últimos seis anos deixaram uma marca na minha formação. Queria agradecer àqueles que me ajudaram diretamente nesse projeto: Carol, Lucas, Dani, Flavio, Juciano e Cami. Sem vocês este projeto não teria acontecido, muito obrigado pela parceria mesmo em tempos de pandemia. Cami, obrigado pela parceria no laboratório e na vida desde a iniciação científica, obrigado pelas incontáveis horas discutindo resultados, experimentos e o futuro. Cresci e aprendi muito contigo, tenho muito orgulho da grande cientista que tu te tornou (do Tiradentes para vida né?). Obrigado também Luciana, pela amizade e por estar sempre por perto nos momentos de incertezas, teu apoio foi essencial.

À professora Maria Elisa, gostaria de agradecer pela oportunidade de ingressar no “mundo” da eletrofisiologia. Por ter me instigado a ampliar meu

conhecimento em Neurociências e ter me acolhido nos teus seminários de grupos desde a graduação. Este projeto de mestrado não seria possível sem o teu apoio e das colegas do laboratório 37. Gostaria deixar meu mais profundo agradecimento a Nati, Querusche e Letícia que em diversas circunstâncias me ajudaram desde as cirurgias de implantação de eletrodos até dúvidas com o Matlab, responderam mensagens domingo pela manhã, marcaram reuniões. Sou extremamente grato por todo auxílio que recebi de vocês.

Gostaria de agradecer também à minha família. Pai, Mãe, o orgulho que sinto de vocês não cabe em palavras. Me sinto extremamente privilegiado pelo esforço e dedicação que vocês aplicaram para prover o melhor possível para mim, para o Matheus e a Helena. O meu sucesso é fruto do amor de vocês, do suporte, do incentivo. Matheus, obrigado pela ajuda com o inglês quando precisei e por demonstrar que se importa e se orgulha, do teu jeito. Helena, obrigado pela convivência e carinho, por ouvir eu treinar para apresentações que tu não entende nada mas ainda assim encontrar alguma pergunta.

Sophia, obrigado meu amor por todas as vezes que tu me escutou falar incessantemente sobre pesquisa (até mesmo as vezes que tu usou isso para dormir). Obrigado por ter ido ao laboratório me ajudar a fazer experimentos. Obrigado por ser a pessoa que mais me entende, por ser meu porto-seguro, minha inspiração. Obrigado por, mesmo com a distância de um oceano, estar sempre ali pra me apoiar. A vida é mais leve contigo, obrigado por existir.

Agradeço também a todos os amigos que vibram e torcem por mim. Andressa, Gui, Roberta, Lucas, Julia vocês ocupam um espaço enorme no meu coração, obrigado por tudo.

Apresentação

O trabalho de mestrado aqui apresentado foi desenvolvido no Centro de Estudos em Estresse Oxidativo, no Departamento de Bioquímica da Universidade Federal do Rio Grande do Sul, sob orientação do Prof. Dr. Daniel Pens Gelain e co-orientação da Profª. Drª. Maria Elisa Calcagnotto. Esta dissertação é apresentada em três partes, onde cada parte é constituída pelos seguintes itens:

Parte I:

Resumo, *Abstract* (versão inglês do resumo), Lista de Abreviaturas, Introdução, Objetivos.

Parte II:

Nesta parte serão apresentados metodologias e resultados na forma de um artigo científico segundo as diretrizes do periódico *Brain Behavior and Immunity.*

Parte III:

Discussão, Conclusão e Perspectivas.

Referências:

As referências bibliográficas não cobertas pela parte II e presentes nas partes I e III serão adicionadas em uma quarta parte.

Anexo I:

Resultados complementares ao trabalho de mestrado; manuscrito submetido ao periódico científico *Neurochemistry International*

Índice

Parte I

Resumo: Uma injeção intraperitoneal de LPS induz uma resposta inflamatória aguda, que eventualmente leva a uma inflamação crônica no cérebro de ratos Wistar. A longo prazo, este estado neuroinflamatório leva a progressiva neurodegeneração no eixo dopaminérgico, deficiência cognitiva e degeneração hipocampal acompanhada por mudanças na vascularização e metabolismo. Nós investigamos se um estímulo inflamatório sistêmico agudo seria capaz de induzir neuroinflamação e neurodegeneração hipocampal e alterações em parâmetros do sono. Ratos Wistar com 50 dias de idade foram tratados com LPS (2mg/kg i.p.) ou salina, 3 ou 5 meses após a injeção foram ou eutanasiados ou submetidos a registros de vídeo-EEG durante o sono. Expressão elevada de citocinas pró-inflamatórias (TNFa e IL1b) e RAGE, somado a níveis elevados do marcador microglial Iba1, da proteína RAGE e atividade de NF-kB, indicam um estado neuroinflamatório 3 meses após o tratamento. Em 5 meses, parâmetros neuro-inflamatórios retornaram aos níveis de controle. Animais tratados demonstraram sinais de neurodegeneração e alterações sinápticas caracterizados por níveis reduzidos de NeuN, NEFL e Sinaptofisina 5 meses após a exposição ao LPS. Apesar de não haver nenhuma diferença entre a percentagem de épocas de sono REM, NREM e vigília, foi possível observar uma redução na duração dos episódios de sono REM. Os picos de Theta e Delta se mantiveram inalterados nas fases de sono REM e NREM, respectivamente, enquanto o poder de Theta durante o sono REM reduziu significativamente 3 meses após o tratamento. Estes resultados indicam que o LPS induz uma neuroinflamação hipocampal crônica capaz de levar a alterações na qualidade do sono REM e neurodegeneração.

Palavras-chave: Neurodegeneração, Inflamação, Sono, LPS, Hipocampo, Doença de Parkinson

Abstract: Intraperitoneal injection of LPS can induce an acute inflammatory response, which eventually leads to sustained brain inflammation in Wistar rats. At length, this neuroinflammatory state leads to progressive neurodegeneration in the dopaminergic axis, cognitive impairment, and hippocampal degeneration accompanied by changes in hippocampal vascularization and metabolism. We investigated whether an acute systemic inflammatory stimulus would induce hippocampal neuroinflammation and neurodegeneration and alter sleep patterns. Fifty-day-old male Wistar rats were treated with LPS (2mg/kg i.p.) or saline, and 3 or 5 months post-injection, they were either euthanized or subjected to video-EEG recordings during sleep. Elevated expression of pro-inflammatory cytokines (TNFa and IL1b) and RAGE, summed by raised levels of microglial marker Iba1, RAGE protein, and NF-kB activity, indicate an environment of hippocampal inflammation 3 months post-injection. In 5 months, neuroinflammatory parameters reached control levels. Treated animals displayed cues of neurodegeneration and synaptic alterations such as diminished levels of NeuN, NEFL, and Synaptophysin 5 months after LPS exposure. Although there were no significant differences between wakefulness (WK), NREM and REM epochs between groups, REM sleep episode duration was reduced 3 months after treatment. Moreover, Theta power diminished significantly during REM sleep 3 months after LPS exposure. Theta and Delta peaks at REM and NREM sleep, respectively, remained unaltered. These results indicate LPS ability to induce chronic hippocampal inflammation which ultimately leads to alterations in REM sleep quality and neurodegeneration.

Keywords: Neurodegeneration, Inflammation, Sleep, LPS, Hippocampus, Parkinson’s Disease

Lista de Abreviaturas

5-HT - 5-hidroxitriptamina

AD - Adrenalina

AMS - Atrofia de Sistema Múltiplos

BBB - *Brain-blood-barrier* (Barreira Hematoencefálica)

CA1 - *Cornus ammonis* 1

Cho - Colina

Cr - Creatina

DA - Dopamina

DCL - Demência com Corpos de Lewy

DOPAC - Ácido 3,4-diidroxifenilacético

DP - Doença de Parkinson

GFAP - Proteína ácida fibrilar glial

Glu - Glutamato

I.P. - Intraperitoneal

Iba1 - Molécula adaptadora ligante de cálcio ionizado-1

IL10 - Interleucina 10

IL1b - Interleucina 1 beta

IL-1R1 - Receptor de Interleucina 1 do tipo 1

IL6 - Interleucina 6

KO - *knockout*

LPS - Lipopolissacarídeo

Myo-Ins - Myo-Inositol

NAA - N-acetil aspartato

NEFL - Neurofilamento Leve

NeuN - Proteína Neuronal Nuclear Específica

NF-kB - Fator nuclear kappa B

NREM - Sono não-REM

PD - *Parkinson's Disease* (Doença de Parkinson)

PRR - *Pattern Recognition Receptor* (Receptor de reconhecimento de padrões moleculares)

PTSD - *Post-traumatic stress disorder* (Perturbação de stresse pós-traumático)

RAGE - Receptor para produtos finais de glicação avançada

RBD - Desordem do Sono REM

REM - Sono com movimento rápido dos olhos

SUS - Sistema Único de Saúde

TH - Tirosina Hidroxilase

TLR4 - Receptor do tipo *toll-like* 4

TNFa - Fator de Necrose Tumoral alfa

TNFR1 - Receptor do Fator de Necrose Tumoral do tipo 1

Introdução

1. Doenças neurodegenerativas no Brasil e no mundo

As Doenças Neurodegenerativas são responsáveis por um número cada vez maior de óbitos ao redor do mundo, afetando uma grande parcela da população mundial acima de 60 anos (Erkkinen et al, 2018). Além do evidente impacto social, desordens neurodegenerativas representam também uma grande ameaça à saúde pública e um enorme fardo econômico (Zahra et al, 2020). Em 2015, o custo estimado do tratamento de demências ao redor do mundo foi de U$818 bilhões (Prince et al, 2015).

Países em desenvolvimento no geral estão vivenciando transições demográficas devido ao aumento da expectativa e qualidade de vida. Essa elevação na idade média da população tem como consequência transições epidemiológicas, incluindo o aumento dos casos de doenças neurodegenerativas progressivas (Burlá et al, 2013). Análises epidemiológicas conduzidas recentemente pelo GBD (GBD 2016 Dementia Collaborators) mostraram a relevância destas doenças para o sistema de saúde brasileiro. Os dados epidemiológicos são espantosos, com o Brasil ocupando um preocupante segundo lugar na prevalência de doenças neurodegenerativas padronizadas pela idade. A maior incidência de desordens neurodegenerativas relacionadas a idade, associadas às cifras exuberantes em torno do tratamento destas doenças, podem aumentar ainda mais a fragilidade do já vulnerável Sistema Único de Saúde - SUS. Dados coletados por Loyola-Filho e colaboradores demonstram que a porcentagem da população SUS-dependente é maior entre os idosos (<60) (Loyola-Filho et al., 2004). Logo, o peso para economia

e sistema de saúde brasileiros em um contexto de aumento da incidência de doenças neurodegenerativas é preocupante.

Os impactos socioeconômicos das desordens neurodegenerativas trazem consigo a necessidade de pesquisa básica focada em revelar os mecanismos por trás dessas doenças, tanto para tratamento quanto para a descoberta de biomarcadores precoces que permitam intervenções em estágios iniciais das doenças, de forma a melhor a qualidade de vida daqueles afetados por estas condições. Neste contexto, diversos preditores de neurodegeneração emergiram, dentre eles destacam-se os distúrbios do sono. No presente trabalho, buscamos identificar se alterações no sono também são percebidas em um modelo animal já estabelecido de neurodegeneração (Qin et al, 2009), na busca por um modelo translacional que nos ajude a compreender as doenças neurodegenerativas, especialmente sinucleinopatias como a Doença de Parkinson (DP).

2. Sinucleinopatias e Distúrbios do Sono

Sinucleinopatias são doenças neurodegenerativas progressivas caracterizadas pelo acúmulo e mal dobramento da proteína alfa-sinucleína (Lotharius et al., 2002). A Doença de Parkinson (DP) e a Demência com Corpos de Lewy (DCL) são caracterizadas por claros déficits locomotores (bradicinesia, tremores e rigidez muscular em repouso) em seus estágios avançados. No estágio prodromal diversos sintomas não-motores podem ser identificados e podem vir a ser boas ferramentas de diagnóstico precoce (Claassen et al, 2010). Na DP, por exemplo, os sintomas motores característicos do diagnóstico clínico desta doença só se tornam evidentes quando o paciente já sofreu uma perda de cerca de 60% dos

neurônios do eixo dopaminérgico enquanto sintomas não-motores como alterações do sono e depressão precedem este quadro de déficits motores (Schapira et al, 2017). Estudos demonstraram que distúrbios do sono como a Desordem do Sono REM (RBD) em sinucleinopatias como a DP, DCL e atrofia de sistemas múltiplos (AMS) pode preceder outros aspectos destas doenças - e seu diagnóstico clínico - por até meio século, com uma mediana de 23 anos entre os primeiros sintomas de RBD e o diagnóstico da sinucleinopatia (Claassen et al, 2010).

Além da degeneração de neurônios do eixo dopaminérgico, outras regiões são acometidas por processos neurodegenerativos em sinucleinopatias. Os núcleos pedunculopontino, locus ceruleus, pontino ceruleus alpha e raphe, centros controladores do sono implicados em desordens do sono REM e NREM, também parecem sofrer perda neuronal em alguns modelos animais da DP (Malhotra et al, 2018). Além disso, a presença de RBD e a severidade dessa desordem em pacientes da DP está diretamente relacionada com um menor volume de regiões subcorticais como o putâmen, o tálamo e o hipocampo (Kamps et al, 2019). A atrofia hipocampal é comum em diversas doenças neurodegenerativas relacionadas a idade e o volume reduzido desta estrutura está diretamente relacionado com uma pior qualidade do sono, eficiência e cansaço diurno (Fjell et al., 2020). Soma-se a isto o fato de que pacientes acometidos com RBD idiopática também apresentam atrofia hipocampal (Campabadal et al., 2019)

3. Relação Inflamação e Sono

Inflamação e sono possuem uma relação de regulação bidirecional (Besedovsky et al., 2019). A relação sono-inflamação é de conhecimento popular; a primeira indicação para uma pessoa acometida por um resfriado é o repouso, e da mesma forma, sabe-se que não dormir horas o suficiente pode levar a um enfraquecimento do nosso sistema imune. Nas últimas décadas, diversos cientistas passaram a buscar esclarecer os mecanismos por trás desta relação. Ao sermos acometidos por infecções - como o resfriado comum - nosso corpo sofre com os desgastes energéticos da febre. De forma adaptativa, diversos comportamentos são alterados coordenadamente - depressão, anorexia, inatividade e sonolência - formando um conjunto que é conhecido como “comportamento de doença” (*sickness behavior*) (Shattuck et al., 2015).

Citocinas pró-inflamatórias estão diretamente ligadas à regulação do sono. IL1b e TNFa possuem sua regulação ligada ao ciclo circadiano e os momentos de maior elevação nos níveis destas citocinas se relacionam com os momentos de máximo sono (Irwin et al., 2017). Além disso, a administração de IL1b ou TNFa promove o sono sem movimento rápido dos olhos (NREM) (Krueger et al., 2008), ademais, níveis elevados destas citocinas suprimem o sono com movimento rápido dos olhos (REM) (Besedovsky et al., 2019). A privação de sono causa como efeito rebote um aumento no sono NREM, tal efeito ocorre concomitante ao aumento da expressão e do conteúdo de IL1b e TNFa; o bloqueio destas citocinas impede este efeito rebote (Irwin et al., 2017). A resposta a mediadores inflamatórios é dose dependente, uma infecção que cause uma inflamação aguda pode gerar a disrupção de ambos sono REM e NREM. Uma infecção induzida por rinovírus leva a uma

redução do tempo total de sono em humanos sintomáticos (Drake et al., 2000). Da mesma forma, sepse induzida por ligadura e punção cecal em ratos leva a disrupção do sono REM e NREM (Baracchi et al., 2011).

4. Neuroinflamação e Neurodegeneração

O acúmulo e mal-dobramento da proteína alfa-sinucleína, leva a formação da principal assinatura patofisiológica das sinucleinopatias: os corpos de Lewy. O mal dobramento e acúmulo de alfa-sinucleína sinaliza para as células gliais disparando uma resposta neuro-inflamatória (Gustot et al., 2015, Lee et al., 2010, Zhang et al., 2005). A inflamação no cérebro, por sua vez, gera um ambiente propício ao mal dobramento de proteínas devido ao aumento da produção de radicais livres (Lipton et al., 2007). Qual estímulo precede o outro na patogênese das sinucleinopatias ainda é um debate aberto, mas é um consenso que tanto o mal-dobramento proteico contribui para a manutenção de um estado inflamatório crônico, como o estado inflamatório contribui para a perpetuação do mal-dobramento proteico (Li et al., 2020, Lema Tomé et al., 2013). Este ciclo de retroalimentação leva a manutenção de um ambiente neurotóxico causando perda neuronal.

As características patofisiológicas da DP e DCL incluem além da formação de corpos de Lewy e perda de neurônios dopaminérgicos, um perfil inflamatório com aumento da ativação glial e infiltração de linfócitos (Glass et al, 2010). Estímulos inflamatórios como patógenos ou padrões moleculares associados a dano são capazes de levar a uma ativação de astrócitos e microglia com capacidades neuroprotetoras (Escartin et al., 2021, Block et al., 2007). No entanto, a super ativação das células gliais leva ao aumento de da produção de radicais livres,

elevada atividade do inflamassoma e NF-kB e acúmulo de mediadores pró-inflamatórios como as citocinas IL1b e TNFa levando a um ambiente neurotóxico (Kwon et al., 2020, Ransohoff et al., 2016, Wyss-Coray et al., 2002).

5. Neurodegeneração Induzida por LPS

Qin e colaboradores caracterizaram o modelo de neurodegeneração induzida por LPS (Qin et al. 2007). Uma única injeção sistêmica de uma alta dose de LPS (5mg/kg i.p.) foi capaz de levar a neuroinflamação crônica e perda neuronal progressiva no eixo dopaminérgico de camundongos C57BL/6J. No mesmo trabalho, os autores observaram que a administração de LPS sistêmico foi capaz de elevar os níveis de TNFa no soro por algumas horas, enquanto os níveis desta citocina no cérebro se mantiveram elevados até 10 meses após o insulto inflamatório. Da mesma forma, também é possível observar ativação microglial na substância negra até 10 meses após a injeção. A elevação destes mediadores inflamatórios no eixo dopaminérgico foi concomitante com uma perda de neurônios tirosina hidroxilase (TH) positivos a partir de 7 meses após a exposição ao LPS. Recentemente, Gasparotto e colaboradores observaram diminuição do imunoconteúdo de TH na substância negra de ratos Wistar tratados com LPS (5mg/kg) em apenas 15 dias após o tratamento com LPS (Gasparotto et al., 2018).

Zhao e colaboradores demonstraram que a exposição crônica ao LPS (injeção diária por 7 dias, 0,750mg/kg) leva a ativação microglial, diminuição dos níveis de citocinas anti-inflamatórias, aumento de mediadores pró-inflamatórios e perda neuronal no hipocampo de camundongos C57BL/6J (Zhao et al., 2019). Towner e colaboradores demonstraram pela utilização de imagem de ressonância

magnética (fMRI) alterações no fluxo sanguíneo cerebral relativo, diminuição de metabólitos do cérebro, disfunção da barreira hemato-encefálica e aumento de radicais livres no hipocampo de ratos expostos a LPS, até 12 semanas após uma injeção intraperitoneal (Towner et al, 2018).

Um insulto inflamatório sistêmico agudo leva a alterações na neurofisiologia do cérebro. Tratamento com LPS é capaz de levar a alterações neuroquímicas no hipocampo de ratos Wistar, caracterizadas por alterações nos níveis de Glu, DA, DOPAC, 5-HT e AD (Náchón-García et al., 2018, Guo et al., 2016). Além disso, o LPS também é capaz de modular a atividade de ondas cerebrais, especialmente alterando parâmetros das oscilações Theta (Mamad et al., 2017). Endotoxemia induzida por LPS também é capaz de diminuir o tempo total do sono REM (Náchón-García et al., 2018).

Tendo em vista a neuroinflamação crônica e progressiva neurodegeneração induzida por LPS, além de sua capacidade de modular a neurotransmissão, ondas cerebrais e sono, buscamos investigar se uma única injeção de uma alta dose de LPS (2mg/kg) seria capaz de levar a neurodegeneração e inflamação no hipocampo, agregado a alterações em parâmetros do sono de ratos Wistar 3 e 5 meses após ao tratamento.

Objetivos do Trabalho

Considerando que o tratamento sistêmico com LPS leva i) a neuroinflamação crônica, ii) a progressiva perda neuronal, iii) modulação de parâmetros neuroquímicos relacionados à neurotransmissão e iv) a modulação de ondas cerebrais e parâmetros do sono; e tendo em vista v) a necessidade de modelos da DP que levem em conta sintomas do estágio prodromal da doença como as alterações do sono, o presente trabalho possui como objetivo **investigar alterações no sono em um modelo de neuroinflamação e neurodegeneração induzida por LPS sistêmico.**

Com o propósito de atingir tal objetivo, iremos avaliar os efeitos da administração sistêmica de LPS em ratos wistar machos de 50 dias de idade, 3 e 5 meses após o tratamento:

a) Avaliar marcadores inflamatórios sistêmicos;
b) Avaliar marcadores inflamatórios no hipocampo;
c) Avaliar marcadores de neurodegeneração e alterações sinápticas no hipocampo;
d) Quantificar o tempo total de permanência em sono REM e sono NREM (fase de sono de ondas lentas);
e) Analisar possíveis variações nos picos das frequências Theta (no sono REM) e Delta (no sono NREM);
f) Analisar o poder das frequências Delta, Theta, Gamma (*Low* Gamma, *High* Gamma e Gamma total) durante o sono REM e NREM.

Parte II

Hippocampal inflammation disrupts REM sleep in a neurodegeneration model induced by systemic LPS

Pedro Ozorio Brum [a], Daniel Oppermann Peixoto [a], Lucas dos Santos Silva [a], Flavio Kessler [a], Carolina Saibro Girardi [a], Camila Tiefensee Ribeiro [a], Natividade de Sá Couto Pereira [b], Querusche Klippel Zanona [b], José Claudio Moreira Fonseca [a], Juciano Gasparotto [a], Cleiton Lopes Aguiar [c], Maria Elisa Calcagnotto [b], Daniel Pens Gelain [a].

[a] Oxidative Stress Research Center (CEEO), Department of Biochemistry, Basic Health Sciences Institute, Federal University of Rio Grande do Sul – Porto Alegre, RS – Brazil;

[b] Neurophysiology and Neurochemistry of Neuronal Excitability and Synaptic Plasticity Laboratory (NNNESP Lab), Department of Biochemistry, Basic Health Sciences Institute, Federal University of Rio Grande do Sul, Porto Alegre, RS, Brazil

[c] Epilepsy Investigations Laboratory, Department of Physiology and Biochemistry, Biological Sciences Institute, Federal University of Minas Gerais, Belo Horizonte MG, Brazil

*Mailing address: Rua Ramiro Barcelos, 2600 – anexo, CEP 90035-003, Porto Alegre, RS, Brazil. Phone: +55 51 3308-5577, Fax: +55 51 3308-5535. E-mail: pedrobrum1@gmail.com

Abstract: Intraperitoneal injection of LPS can induce an acute inflammatory response, which eventually leads to sustained brain inflammation in Wistar rats. At length, this neuroinflammatory state leads to progressive neurodegeneration in the dopaminergic axis, cognitive impairment, and hippocampal degeneration accompanied by changes in hippocampal vascularization and metabolism. We investigated whether an acute systemic inflammatory stimulus would induce hippocampal neuroinflammation and neurodegeneration and alter sleep patterns. Fifty-day-old male Wistar rats were treated with LPS (2mg/kg i.p.) or saline, and 3 or 5 months post-injection, they were either euthanized or subjected to video-EEG recordings during sleep. Elevated expression of pro-inflammatory cytokines (TNFa and IL1b) and RAGE, summed by raised levels of microglial marker Iba1, RAGE protein, and NF-kB activity, indicate an environment of hippocampal inflammation 3 months post-injection. In 5 months, neuroinflammatory parameters reached control levels. Treated animals displayed cues of neurodegeneration and synaptic alterations such as diminished levels of NeuN, NEFL, and Synaptophysin 5 months after LPS exposure. Although there were no significant differences between wakefulness (WK), NREM and REM epochs between groups, REM sleep episode duration was reduced 3 months after treatment. Moreover, Theta power diminished significantly during REM sleep 3 months after LPS exposure. Theta and Delta peaks at REM and NREM sleep, respectively, remained unaltered. These results indicate LPS ability to induce chronic hippocampal inflammation which ultimately leads to alterations in REM sleep quality and neurodegeneration.

Keywords: Neurodegeneration, Inflammation, Sleep, LPS, Hippocampus, Parkinson’s Disease

Highlights

- Systemic LPS induces hippocampal neuroinflammation characterized by elevated levels of Iba1, RAGE, and NF-kB activity;
- NF-kB activation leads to increased expression of pro-inflammatory cytokines IL1b and TNFa within the hippocampus;
- Sustained neuroinflammation leads to diminished levels of neuronal markers NeuN and NEFL as well as reduced levels of synaptic related protein Synaptophysin;
- Temporal correlation between elevated levels of inflammatory mediators and alterations in REM sleep parameters is observed in LPS treated animals.

1. Introduction

Parkinson's Disease (PD) is a progressive neurological disorder that causes the loss of dopaminergic neurons of the basal ganglia, ultimately leading to severe motor deficits (Lotharius et al., 2002). Although its pathogenesis is not yet fully comprehended, it is believed that several factors play a role in this disease, such as protein misfolding and accumulation (Stefanis et al. 2012), mitochondrial dysfunction (Park et al., 2018), and neuroinflammation (Kwon et al., 2020). Summed to movement disorders, it is notable the presence of non-motor features of the disease. Insomnia, Excessive Daytime Sleepiness (EDS), and REM Sleep Behavior Disorder (RBD) are a few non-motor symptoms that most PD patients have to coexist with (Schapira et al., 2017). RBD, for instance, may precede motor deficits by several decades (Claassen et al., 2010). Besides, PD patients presenting RBD demonstrate a diminished volume of subcortical areas such as the hippocampus, hypothalamus, and putamen (Kamps et al., 2019). Several authors have demonstrated the relevance of sleep alterations to signalize risk population and disease progress (Bohnen et al., 2019, Suzuki et al., 2017, Claassen et al., 2010). Animal models capable of reproducing non-motor features of this disease will help understand the neurodegenerative processes involved in PD.

Lipopolysaccharide (LPS) is a component of the cell membrane of gram-negative bacteria. This molecule can initiate an inflammatory response by activating Pattern Recognition Receptors (PRRs) such as the receptor for advanced glycation end-products (RAGE) and toll-like receptor 4 (TLR4), thus releasing proinflammatory cytokines such as Interleukin-1b (IL1b) and tumor necrosis factor-a (TNFa) (Lu et al., 2008, Gasparotto et al., 2017). A single high-dose Intraperitoneal

injection of LPS induces a process of endotoxemia similar to sepsis in Wistar rats (Buras et al., 2005, Opal et al., 2010). An acute inflammatory stimulus by LPS exposure ultimately leads to damage to the brain-blood-barrier (BBB), glial activation, and a sustained neuroinflammatory state, which becomes neurotoxic (Qin et al., 2007, Gasparotto et al., 2017, Towner et al., 2018, Zhao et al., 2019). LPS-induced neuroinflammation leads to a reduction of Tyrosine Hydroxylase (TH) positive neurons in the substantia nigra (Qin et al. 2007), induces alterations in vascularity, a decrease in brain metabolites, and increased free radicals in the hippocampus (Towner et al., 2018); chronic exposure to systemic LPS promotes cognitive impairments and neuronal loss in the hippocampus of C57BL/6J mice (Zhao et al., 2019)

Inflammation and sleep have mutual regulatory mechanisms (Irwin et al., 2017). Cytokines, both pro-inflammatory and anti-inflammatory, influence sleep homeostasis. IL1b and TNFa have been described as promoters of Not-Rapid-Eye-Movement (NREM) sleep (Besedovsky, 2019). These cytokines physiologically vary during the sleep-wake cycle, and cytokine peaks seem to be influenced by circadian regulators (Besedovsky, 2011). Central administration of pro-inflammatory cytokine IL1b leads to suppressed REM sleep (Ingiosi, 2014). While these pro-inflammatory mediators' physiological levels induce non-rapid eye movement (NREM) sleep and reduce rapid eye movement (REM) sleep duration, higher levels of cytokines may disrupt both brain states (Opp et al., 1991). Besides, anti-inflammatory cytokines IL4, IL10, and IL13 attenuate NREM sleep (Kushikata et al., 1998, Kushikata et al., 1999, Kubota et al., 2000). Acute inflammation alters brain waves and sleep patterns. Sepsis-induced by cecal ligation and puncture (CLP) in Wistar rats reduces REM sleep in the first 84h post-procedure (Baracchi et al., 2011).

Meanwhile, LPS treated animals demonstrate a reduction of REM sleep in the first 4h post insult (Nachón-García et al., 2018).

Considering the aforementioned capacity of a systemic injection of LPS in inducing chronic neuroinflammation and neurodegeneration, the role of inflammatory mediators in the regulation of sleep homeostasis, and the correlation between neurodegeneration and sleep alterations, we investigated the effects of a high-dose intraperitoneal injection (2 mg/kg) of LPS in inflammatory and neurodegenerative markers within the hippocampus. Moreover, we assessed the time spent in each brain state during sleep, REM, NREM sleep (Slow-Wave phase) and Wakefulness (WK) and the duration of each episode. Hippocampal power of Delta, Theta, and Gamma (Low Gamma, High Gamma and total Gamma) frequencies were quantified during REM and NREM sleep. We also assessed peak Delta frequency during NREM sleep and peak Theta frequency during REM sleep.

2. Methods

2.1 Ethics Statement

The research protocol was approved under project number **37193** by the Ethical Committee for Animal Experimentation of the Universidade Federal do Rio Grande do Sul, Brazil (CEUA-UFRGS). All experimental procedures were performed according to the Brazilian Society for Neuroscience and Behavior recommendations for animal care. All efforts have been made to minimize animal suffering.

2.2 Animals

One hundred and forty Male Wistar rats (50 days-old) were obtained in the Laboratory Animal Reproduction and Experimentation Center of the Universidade Federal do Rio Grande do Sul, Brazil (CREAL-UFRGS). Animals were caged in groups of 4 animals with free access (*ad libitum*) to water and food (Chow Nuvilab CR-1 type; PR, Brazil). Animals were maintained at constant room temperature of 21 ± 1 °C in a 12-h light-dark cycle.

2.3 Experimental Design

Thirty six animals were used to perform a dose curve with three different concentrations of LPS (Sigma-Aldrich®, Cat. O111:B4). The dose of 2mg/kg was selected with a survival rate of 53.3% (sup. fig. 1). Animals were then randomly divided between LPS and Control. Treated animals received a single intraperitoneal injection of LPS 2 mg/kg (n= 70). Control animals received an i.p. injection of saline (n= 35). LPS treatment resulted in the loss of 37 animals. Stereotaxic surgery for electrode implantation was performed in 38 animals. Eighteen of these animals were discarded from analysis either because of complications during surgery or wrongful electrode implantation. Animals selected for Western Blot and RT-qPCR were euthanized by decapitation (n= 10 per group). Serum was collected and the hippocampus was isolated. Animals that underwent Video-EEG recordings (n= 5 per

group) were intracardially perfused for confirmation of electrode position through histology (Fig. Sup. 1).

2.4 Enzyme-linked immunosorbent assay (ELISA)

Serum cytokines (IL1b, IL10, and IL6) were evaluated through indirect ELISA (n= 8 per group). Samples were incubated overnight in 96 well-plates and then washed three times with Tween-Tris buffered saline (TTBS, 100 mM Tris – HCl, pH 7.5, containing 0.9%NaCl, and 0.1% Tween-20). Subsequently, 200uL of primary antibody (Table S1) was added and incubated for 24 h at 4°C. The plates were washed three times with TTBS and incubated with the respective peroxidase-linked secondary antibody (1:1000) for 2 h. After washing the plate three times with TTBS, 200µL of substrate solution (TMB spectrophotometric ELISA detection kit) were added to each well and incubated for 15 min. The reaction was terminated with 50µL/well of 12M sulfuric acid stopping reagent, and the plate read at 450 nm in a microplate. The results are expressed as percentage of control. TNFa levels were measured using a commercial kit (KRC3011, Invitrogen) (n= 6 per group) following the manufacturer's instructions.

2.5 Western Blot

Hippocampal samples were homogenized in the RIPA buffer (150 mM sodium chloride, 1.0% NP-40, 0.5% sodium deoxycholate, 0.1% SDS, 50 mM Tris, pH 8.0). Total protein was quantified by Bradford assay, and samples were normalized with a

Laemmli buffer (250 mM Tris, 8% SDS, 40% glycerol, and 0.002% bromophenol blue, pH 6.7). Samples were vigorously vortexed and boiled for ten minutes at 100°C. Samples were loaded (20µg/µl) and separated in 10% polyacrylamide gel and then electro-blotted to nitrocellulose membranes. Protein loading and electroblotting efficiency were verified through Ponceau S staining. Membranes were washed in Tris-buffered saline Tween-20 (Tris 100 mM, pH 7.5, 0.9% NaCl and 0.1% Tween-20) and blocked in TBS-T with 5% BSA. Membranes were washed three times post-blocked and then incubated overnight at 4°C with primary antibodies (all primary antibodies were used at 1:1000 dilution) for NeuN, NEFL, Synaptophysin, PSD95, Iba1, GFAP, S100b, RAGE, p65, p-p65 and β-actin (Table S1). Subsequently, membranes were incubated with the corresponding species-specific secondary antibody (all secondary antibodies were used at 1:2000 dilution) coupled to peroxidase (Sigma-Aldrich - AP132P; AP124P) following chemiluminescence detection utilizing the Westar Nova 2.0 kit (Cyanagen - XLS071,0250) and the GE® ImageQuant LAS 4000 CCD camera to obtain images.

2.6 Real Time-qPCR

Samples were homogenized utilizing the TRIzol reagent (Thermo Fisher Scientific) and RNA extractions were conducted following the manufacturer's instructions. cDNA synthesis was performed using the High Capacity cDNA Reverse Transcription kit from Applied Biosystems. Real-time polymerase chain reaction was carried employing SYBR™ Green PCR Master Mix kit, 100 ng of cDNA and 100µM of each primer: *IL1b*, *TNFa*, *IFNg*, *RAGE*, and the housekeeping genes *GNB2L* and *B2M* (Table S2). Results were normalized to the housekeeping genes (ΔCt) and the

most stable housekeeping gene was applied. Results were expressed using the $2^{-\Delta\Delta CT}$ method.

2.7 Stereotaxic Surgery

Three or five months after LPS injection electrode placement was performed (n= 38), animals were anesthetized with ketamine/xylazine (100 mg/kg/10 mg/kg, i.p.). Animals were fixed in a stereotaxic and bilateral intrahippocampal electrodes were implanted (LL= ±2.5mm, AP=-3.6mm DV=-2.5mm). A subdural electrode placed in the occipital area was used as a reference. An electrode was placed in the neck muscle to assess electromyographic (EMG) activity. Electrodes were fixed with dental cement. Animals were caged in new boxes (1 animal/box) and allowed to recover for 5 to 7 days after electrode implantation. After recordings animals were anesthetized and intracardially perfused. Brains were fixed at 4% PFA and maintained at 30% sucrose. 80um slices were acquired using a VTS-1000, Leica vibratome. Hematoxylin and Eosin (HE) staining was performed to confirm the correct placement of electrodes.

2.8 Electrophysiological Recordings and Analysis

All animals were acclimated to the recording site 2 to 3 days before the recordings. Electrodes were then connected to a Video-EEG system (MAP-23, Plexon inc. - sample rate of 1000 Hz; bandpass filter 0,1-500 Hz; preamp gain 1000 Hz). No significant differences between left and right hippocampal electrodes were observed (Fig S2); therefore, analysis does not discriminate between sides. Five

hours length recordings were performed during the daylight phase. 300 epochs of 10sec each were analyzed and classified as Non-Rapid-Eye-Movement Sleep (NREM), Rapid-Eye-Movement Sleep (REM), or Wakefulness (WK). Recordings were analyzed employing custom-written routines in MATLAB (Mathworks). EMG Root mean square was assessed to define muscular atonia epochs. Power spectral density (PSD) was estimated using *pwelch* and power was normalized by total frequency power (1-100Hz). Data were clusterized through a k-means algorithm (squared Euclidean distance for three groups) and visually inspected. **Atonia** epochs were classified as REM or NREM accordingly to: Theta/Delta power > 1 = REM or Theta/Delta power < 1 = NREM (Lopes-Aguiar et al., 2020). **Movement** epochs were defined as Wakefulness (WK). Epochs in which Theta/Delta ≅ 1 or in the cluster edges were disregarded to avoid misclassification. Unclassified epochs were disregarded for analysis. Frequency bands were classified as Delta (1-4Hz), Theta (5-10Hz), Low Gamma (25-55Hz), High Gamma (65-100Hz), and Gamma (25-100Hz). Delta and Theta peak frequency were defined as the discrete frequency with the highest magnitude within the range of the analyzed frequency. Time spent in each brain state was estimated as a percentage of total epochs analyzed for every animal. Episode duration was assessed as the average time (sec) necessary to switch to another brain state. Animal immobility was confirmed through video analysis.

2.9 Statistical Analysis

Statistical analysis was performed with the GraphPad Prism software version 7.0 (GraphPad Software Inc., San Diego, USA). Normality was assessed through the

D'Agostino-Pearson test. Data were considered non-parametric and evaluated by Kruskal-Wallis test followed by Dunn's *post-hoc* test. Differences were considered significant when $p<0.05$.

3. Results

3.1 Cytokine levels in serum remained unaltered

Levels of circulating cytokines were quantified in the serum of control and LPS-treated animals by ELISA. There were no significant differences in levels of the proinflammatory cytokines TNFa (n= 6 per group), IL6, IL1b, and anti-inflammatory IL10 (n= 8 per group) (Fig 1). These results were expected, as cytokines clearance half-lives may vary from 8h to 24h (Kuribayashi et al., 2018, Leelahavanichkul et al., 2011). Furthermore, as previously reported by other authors, inflammatory exacerbation of the Central Nervous System in LPS models is independent of circulating cytokines (Murray et al., 2011) and serum TNFa levels do decay to control levels within the first 24h post-injection while brain TNFa levels remained elevated months after the inflammatory insult (Qin et al., 2007).

Therefore, inflammation-related gene expression and biochemical markers of neuroinflammation were further analyzed in the hippocampus of Control and LPS-treated animals to characterize the neuroinflammatory status.

3.2 Systemic LPS exposure induced a neuroinflammatory state

Whereas hippocampal levels of GFAP and S100b (Fig 2B-C) - astrocyte markers - were unaltered, Iba1 (Fig 2A) - microglial marker - levels were significantly increased 3 months after LPS treatment. Elevated immunocontent of RAGE and increased phosphorylation of p65 (NF-kB) were also observed 3 months post-injection (n= 6 per group). Expression of pro-inflammatory cytokines TNFa and IL1b was elevated in the hippocampus 3 months after LPS exposure (Fig. 3A-B). RAGE expression remained elevated 3 and 5 months post-injection. INFg expression remained unaltered (n= 7 per group).

These alterations suggest a neuroinflammatory environment with microglial pro-inflammatory phenotype within the hippocampus of LPS treated rats 3 months post-injection. Such a profile was not sustained 5 months post-injection.

3.3 LPS leads to diminished levels of neuronal markers and synapse related protein Synaptophysin

Whereas Qin and collaborators were capable of detecting increased neurodegeneration of nigral dopaminergic neurons only 7 months after a single dose of LPS (Qin et al., 2007), new investigations have shown diminished TH levels in the *substantia nigra* as early as 15 days after treatment (Gasparotto et al., 2017). Moreover, 7 consecutive high-dose daily injections of LPS were capable of altering neuroinflammatory and neuronal markers in mice hippocampus within 7 days (Zhao et al., 2019). Therefore, we evaluated protein levels related to neurodegeneration in rats hippocampus through western blot analysis (Fig 4) (n= 6 per group).

While levels of PSD95 (Fig 4C) showed no relevant changes, NeuN (Fig 4A), NEFL (Fig 4B), and Synaptophysin (Fig 4D) levels demonstrated a significant decrease 5 months after LPS treatment. Such findings suggest that a sustained pro-inflammatory state within the hippocampus induced by a single high-dose i.p. injection of LPS leads to neuronal loss and synaptic disruption in older ages (5 months) rather than younger ages (3 months).

3.4 Reduced REM sleep episode duration without changes in total sleep time or frequency peak

Inflammation (Besedovsky et al., 2019) and neurodegeneration (Malhotra et al., 2018) within the brain are strictly related to sleep pattern alterations. Herewith, we wanted to address whether a sustained pro-inflammatory environment would induce alterations in sleep patterns.

Therefore, LPS treated animals (n= 5 per group) were recorded during sleep for 5 hours within the day light-phase (Fig 5A). There were no relevant changes in time spent in WK, NREM and REM sleep either 3 months (Fig 5B) or 5 months (Fig 5C) post-injection. However, REM sleep episode duration was significantly decreased (p= 0,0403) 3 months after LPS treatment (Fig 5D). WK, NREM and REM episode duration remained unaltered 5 months post-injection.

Peak theta frequency during REM sleep (Fig 5B) and peak delta frequency during NREM sleep (Fig 5C) were assessed. A clear delta peak of 2,212Hz ± 0,099 was observed for Control 3 months (n= 5), 2,112 ± 0,464 for Control 5 months (n= 5), 2,095Hz ± 0,237 for LPS 3 months (n= 5) and 2,242 ± 0,241 for LPS 5 months (n= 5). No differences were observed between groups. A theta peak was observed at 6,615

± 0,352 for Control 3 months (n= 5), 6,537 ± 0,384 for Control 5 months (n= 5), 7,06 ± 0,468 for LPS 3 months (n= 5) and 6,752 ± 0,172 for LPS 5 months (n= 5). It was not possible to detect any significant alteration.

3.5 Systemic LPS induces reduction of hippocampal power spectral density of Theta oscillation during REM sleep

Inflammatory mediators affect brain wave activity. TNFa and IL1b central or systemic injections increase delta wave activity during NREM (Krueger et al.,2008). LPS treated 3–6 months old male Lister-Hooded rats demonstrate a reduction of PSD of hippocampal Delta and Theta oscillation in the first 24h after an inflammatory insult (Mamad et al., 2017). Therefore, we assessed if chronic hippocampal neuroinflammation induced by LPS was capable of altering brain wave activity during REM or NREM.

PSD of Delta, Low Gamma, High Gamma and total Gamma oscillations showed no significant differences across brain states and treatments (Fig 6). In LPS treated animals PSD of Theta oscillation was significantly reduced 3 months (p=0,0277) after a systemic inflammatory insult and returned to control levels at 5 months (Fig 6D).

4. Discussion

In the present study, it was possible to observe a temporal correlation between increased inflammatory parameters in the hippocampus and a reduction in REM sleep PSD of theta oscillations and episode duration 3 months after an acute

systemic inflammatory stimulus. 5 months after exposure was possible to observe a reduction in neuronal markers and the synapse-related protein Synaptophysin levels. These results indicate that a systemic injection of LPS can induce chronic neuroinflammation, REM sleep alterations, and hippocampal degeneration.

4.1 Chronic hippocampal inflammation induced by systemic LPS

Systemic LPS leads to a sepsis-like state in animal models (Buras et al., 2005, Opal et al., 2010). Systemic cytokine levels peak and decay within the first 24h after LPS exposure (Qin et al., 2007, Gasparotto et al., 2017). However, this insult leads to damage to the BBB, allowing infiltration of inflammatory mediators in the brain and cerebrospinal fluid (Gasparotto et al., 2017). These molecules in the brain lead to microglial activation and subsequent increase of pro-inflammatory cytokines in the brain (Hoogland et al., 2015).

Besides, the pattern recognition receptor RAGE changes its site of expression from vascular endothelial cells to neurons in response to LPS treatment (Gasparotto et al., 2019), allowing the perpetuation of this inflammatory state through activation of NF-kB and increasing the expression of RAGE itself (Somensi et al., 2017). RAGE is a pattern recognition receptor which interacts with a wide range of different molecules linked to infection and tissue damage (Fritz et al., 2011, Kierdorf et al., 2013). RAGE expression is induced by pro-inflammatory cytokines such as TNFa (Tanaka et al., 2000). In this work, systemic LPS treatment was capable of increasing neuroinflammatory parameters 3 months after exposure. Increase in RAGE protein and expression levels (Fig 2D, Fig 3C), summed to elevated phosphorylation of NF-kB (Fig 2E) and high expression of TNFa and IL1b (Fig 3A-B), summed to

elevated levels of Iba1 (Fig 2A), indicate that systemic LPS treatment triggers RAGE signaling in the brain, leading to a inflammatory state with the presence of reactive microglia.

Qin and collaborators have demonstrated increased microglial activation and elevated levels TNFa in the *substantia nigra* of C57BL/6J mice 10 months after LPS exposure (Qin et al., 2007). Towner and collaborators have reported a decrease in the N-acetyl aspartate/choline (NAA/Cho) ratio in the hippocampus 3 months after LPS injection in Wistar rats (Towner et al., 2018). Elevated levels of Cho and reduced levels of NAA are linked to astrogliosis, inflammation, and early axonal degeneration (Mader et al., 2008). The authors also observed a decrease in Creatine/Cho (Cr/Cho) and Myo-inositol/Cho (Myo-ins/Cho) ratios (Towner et al., 2018), both indicators of astrogliosis and inflammation (Kendall et al., 2014, Kim et al., 2005). Despite inflammation being persistent for up to 3 months in the hippocampus, some results suggest that it might not endure as long as neuroinflammation in the *substantia nigra*. Hippocampal Myo-inositol/Cho ratio, BBB impairments, and relative cerebral blood flow return to control levels after 3 months, and free radicals production normalize past 1 week (Towner et al., 2018); as observed in our experiments, Iba1 levels, NF-kB phosphorylation, and expression of IL1b and TNFa return to control levels 5 months after LPS exposure. Structure-specificity of the immune response and differences in glial cell density might be responsible for the differences in inflammation maintenance.

4.2 Chronic neuroinflammation causes neuronal loss and synaptic alterations

Neuroinflammation, defined as a collective of alterations within the brain, including glial activation and secretion of inflammatory mediators, is one of the leading environmental features of neurodegenerative disorders responsible for the generation of a neurotoxic environment (Ransohoff et al., 2016). Neuroinflammation is a defense mechanism that protects the brain from damage and pathogens (Wyss-Coray et al., 2002). However, chronic neuroinflammation, with persistent microglial and astrocytic inflammatory phenotypes, inhibits regeneration (Russo et al., 2016, Kempuraj et al., 2016) and promotes neuronal loss (Qin et al., 2007, Gasparotto et al., 2018, Zhao et al., 2019).

Customarily, glial cells are classified in a dichotomic manner, either as a neurotoxic pro-inflammatory phenotype (M1 for reactive microglia, A1 for reactive astrocyte) or protective (M2 for regulatory microglia, A2 for regulatory astrocyte). It is appealing to use such simplified classifications; however, they don't reflect the reality. Microglial and astrocytic phenotypes should be classified in a spectrum rather than in a binary form (Kwon et al., 2020, Escartin et al., 2021). GFAP is widely used as a marker of reactive astrocytes. Although, elevated levels of GFAP are not definitive markers of a pro-inflammatory phenotype (Escartin et al., 2021). GFAP levels vary between brain structures; for instance, GFAP positive cells' density is higher in the hippocampus (Haim et al., 2017). Iba1 is commonly used as a microglial activation marker, although its expression is related to all microglia (Hopperton et al., 2018). In both cases, proliferative markers should be used to confirm recruitment and proliferation of glial cells (Kwon et al., 2020, Escartin et al., 2021). Therefore, changes in these markers alone do not represent glial activation and cannot be linked

to either a protective or neurotoxic state. Nevertheless, the increase of other inflammatory parameters observed (NF-kB phosphorylation, increased expression of IL1 and TNFa) provides evidence of a neurotoxic environment induced by LPS treatment.

Microglia represent ~12% of the cells in the brain with a variety of different densities across brain regions (0,5% - 16,6%); regions such as de basal ganglia and the hippocampus have a high density of microglia (Block et al., 2007). Several stimuli are capable of activating microglia triggering major alterations in cell morphology and function (Nimmerjahn et al., 2005, Fetler et al., 2005). Activation of microglia serves several purposes in neuronal protection - “environmental surveillance” (clearance of neurotoxic molecules in the cytoplasm), neuronal survival through release of trophic and anti-inflammatory mediators and innate immune response (Simard et al., 2006, Town et al., 2005, Liao et al., 2005, Streit et al., 2002). Although, overactivation of microglia becomes neurotoxic leading to increased production of free radicals, elevated activity of NF-kB and the inflammasome, and a rise in levels of pro-inflammatory cytokines (Kwon et al., 2020, Ransohoff et al., 2016, Wyss-Coray et al., 2002).

4.3 Neuroinflammation disrupts REM sleep

REM sleep is characterized by a predominance of Theta waves in hippocampal LFP recordings, muscular atony, rapid eye movement, and a clear peak around 7Hz during its tonic phase (Jing et al., 2016). NREM is characterized by an alternance between periods of spiking (UP state) and periods of hyperpolarization with large “slow waves” (SW phase) with a predominance of Delta wave activity in

hippocampal LFP recordings, muscular atony, absence of rapid eye movement, and a clear peak around 2Hz (Levenstein et al., 2019, Jing et al., 2016). Changes in inflammatory mediators levels, due to physiological variation triggered by circadian clock proteins or induced by an inflammatory insult, modulate sleep homeostasis (Besedovsky et al., 2019).

Inflammatory mediators affect brain wave activity. LPS treated 3–6 months old male Lister-Hooded rats demonstrate a reduction of hippocampal Delta and Theta frequency and Theta peaks in the hippocampus show a considerable reduction in the first 24h after an inflammatory insult (Mamad et al., 2017). Meanwhile, sepsis through CLP and endotoxemia by LPS disrupt REM sleep (Baracchi et al., 2011, Nachón-García et al., 2018). TNFa and IL1b central or systemic injections increase delta wave activity during NREM (Krueger et al.,2008). Moreover, IL1b and TNFa elevated levels induce NREM sleep and disrupt REM sleep (Besedovsky et al., 2019). When exposed to sleep deprivation, control mice present prolonged NREM and REM sleep; moreover, IL-1R1 and TNFR1 KO mice cannot compensate for the sleep loss through an increase in sleep time. Although, no changes in the time spent in each brain state are observed (Baracchi et al., 2008). Also, IL-1R1 KO mice are not responsive to CA1 theta-burst stimulation (Avital et al., 2003). In the present study, we observed a temporal correlation between increased neuroinflammatory parameters, reduced REM sleep epochs and hippocampal REM PSD of theta oscillations. Meanwhile, there were no changes in Delta and Theta frequencies peak. Our results suggest that pro-inflammatory cytokines cause REM sleep fragmentation and modulate theta oscillation activity during REM sleep months after LPS exposure.

Coherence between hippocampal theta activity and amygdala theta activity triggers gene expression related to plasticity, indicating a role for REM sleep in

emotional memory consolidation (Hutchison et al., 2015). Synaptophysin is a presynaptic protein, and reduction in its levels is directly related to alterations in plasticity-related mechanisms such as loss of long-term potentiation (LTP) (Li et al., 2012, Janz et al., 1999). LTP is a relevant mechanism of plasticity and memory consolidation (Lynch et al., 2004). Previous studies have demonstrated cognitive and memory impairments in LPS treated animals (Zhao et al., 2019, Joshi et al., 2015).

REM and NREM fragmentation without alterations in total sleep have implications in emotional memory fear consolidation (Lee et al., 2016). Moreover, adult neurogenesis is also afflicted by LPS treatment (Perez-Domingues et al., 2019). Although adult-born neuron inhibition does not affect REM sleep or theta power, their sparse activity during REM sleep is highly relevant to fear memory consolidation (Kumar et al., 2020). Furthermore, REM sleep fragmentation has implications in psychiatric disorders such as depression and Post-traumatic stress disorder (PTSD) (Lipinska et al., 2019, Pesonen et al., 2019). LPS-treated animals displayed a reduction in REM sleep episode duration - without alterations in total sleep - 3 months post-injection. Further behavioral analysis might provide insights on the effects of LPS-induced REM sleep disruption on brain plasticity and behavior.

Previous studies have demonstrated that hippocampal injury affects sleep quality (Spanò et al., 2020); conversely, sleep deprivation caused by sleep apnea impairs hippocampal function and adult neurogenesis (Navarro-Sanchis et al., 2017, Mueller et al., 2008). Idiopathic RBD patients present hippocampal atrophy (Campabadal et al., 2019). Depression is one of the significant non-motor features of Parkinson's Disease, afflicting around 50% of the patients (Reijnders et al., 2008). Hippocampal atrophy is linked to the severity of Depressive Disorders' clinical features (Sheline et al., 2011). Sleep and depression, relevant prodromal features of

Parkinson's Disease, relate to hippocampal atrophy and degeneration. However, many models of Parkison's Disease tend to ignore the relevance of processes of degeneration occurring in structures outside the dopaminergic axis (Tieu et al., 2011). Therefore, it is necessary to address all dysfunctions caused across brain regions to properly model this disease and tackle the many questions that have been puzzling researchers since the first description of Parkison's Disease.

5. Conclusion

LPS treatment induces a neuroinflammatory state in the hippocampus of 50 days old Wistar rats 3 months after exposure. Brain inflammation is characterized by increased Iba1, RAGE, NF-kB activity, and elevated expression of the proinflammatory cytokines IL1b and TNFa. These cytokines are strictly related to the modulation of sleep patterns. High levels of these inflammatory mediators have a temporal correlation with reduced duration REM sleep episodes and with reduced PSD of Theta oscillation during REM sleep. That indicates a disruption of REM sleep even months after systemic LPS exposure attributed to a chronic neuroinflammatory state. Inflammatory and sleep parameters returned to control levels 5 months after treatment.

Meanwhile, neurodegeneration and synaptic alterations were observed in the hippocampus of treated animals. These features were characterized by reduced levels of NEFL, NeuN, and Synaptophysin. These results highlight the possibility of using alterations of sleep and inflammatory parameters to indicate risk populations

for neurodegenerative disorders and the possibility of translation of such features to animal models.

6. Conflicts of interest

The authors declare no conflicts of interest

7. Funding Sources

This study was supported by Conselho Nacional de Desenvolvimento Científico e Tecnológico (CNPq), FAPERGS, Propesq-UFRGS and Coordenação de Aperfeiçoamento de Pessoal de Nível Superior (CAPES).

8. References

1. Avital A, Goshen I, Kamsler A, Segal M, Iverfeldt K, Richter-Levin G, Yirmiya R. Impaired interleukin-1 signaling is associated with deficits in hippocampal memory processes and neural plasticity. Hippocampus. 2003;13(7):826-34. doi: 10.1002/hipo.10135. PMID: 14620878.
2. Baracchi F, Ingiosi AM, Raymond RM Jr, Opp MR. Sepsis-induced alterations in sleep of rats. Am J Physiol Regul Integr Comp Physiol. 2011 Nov;301(5):R1467-78. doi: 10.1152/ajpregu.00354.2011. Epub 2011 Sep 7. PMID: 21900639; PMCID: PMC3213944.
3. Baracchi F, Opp MR. Sleep-wake behavior and responses to sleep deprivation of mice lacking both interleukin-1 beta receptor 1 and tumor necrosis

factor-alpha receptor 1. Brain Behav Immun. 2008 Aug;22(6):982-93. doi: 10.1016/j.bbi.2008.02.001. Epub 2008 Mar 7. PMID: 18329246; PMCID: PMC4164115.

4. Ben Haim L, Rowitch DH. Functional diversity of astrocytes in neural circuit regulation. Nat Rev Neurosci. 2017 Jan;18(1):31-41. doi: 10.1038/nrn.2016.159. Epub 2016 Dec 1. PMID: 27904142.
5. Besedovsky L, Lange T, Born J. Sleep and immune function. Pflugers Arch. 2012 Jan;463(1):121-37. doi: 10.1007/s00424-011-1044-0. Epub 2011 Nov 10. PMID: 22071480; PMCID: PMC3256323.
6. Besedovsky L, Lange T, Haack M. The Sleep-Immune Crosstalk in Health and Disease. Physiol Rev. 2019 Jul 1;99(3):1325-1380. doi: 10.1152/physrev.00010.2018. PMID: 30920354; PMCID: PMC6689741.
7. Block ML, Zecca L, Hong JS. Microglia-mediated neurotoxicity: uncovering the molecular mechanisms. Nat Rev Neurosci. 2007 Jan;8(1):57-69. doi: 10.1038/nrn2038. PMID: 17180163.
8. Bohnen NI, Hu MTM. Sleep Disturbance as Potential Risk and Progression Factor for Parkinson's Disease. J Parkinsons Dis. 2019;9(3):603-614. doi: 10.3233/JPD-191627. PMID: 31227656; PMCID: PMC6700634.
9. Buras JA, Holzmann B, Sitkovsky M. Animal models of sepsis: setting the stage. Nat Rev Drug Discov. 2005 Oct;4(10):854-65. doi: 10.1038/nrd1854. PMID: 16224456.
10. Campabadal A, Segura B, Junque C, Serradell M, Abos A, Uribe C, Baggio HC, Gaig C, Santamaria J, Compta Y, Bargallo N, Iranzo A. Cortical Gray Matter and Hippocampal Atrophy in Idiopathic Rapid Eye Movement Sleep

Behavior Disorder. Front Neurol. 2019 Apr 5;10:312. doi: 10.3389/fneur.2019.00312. PMID: 31024418; PMCID: PMC6459930.

11. Claassen DO, Josephs KA, Ahlskog JE, Silber MH, Tippmann-Peikert M, Boeve BF. REM sleep behavior disorder preceding other aspects of synucleinopathies by up to half a century. Neurology. 2010 Aug 10;75(6):494-9. doi: 10.1212/WNL.0b013e3181ec7fac.
12. Escartin C, Galea E, Lakatos A, O'Callaghan JP, Petzold GC, Serrano-Pozo A, Steinhäuser C, Volterra A, Carmignoto G, Agarwal A, Allen NJ, Araque A, Barbeito L, Barzilai A, Bergles DE, Bonvento G, Butt AM, Chen WT, Cohen-Salmon M, Cunningham C, Deneen B, De Strooper B, Díaz-Castro B, Farina C, Freeman M, Gallo V, Goldman JE, Goldman SA, Götz M, Gutiérrez A, Haydon PG, Heiland DH, Hol EM, Holt MG, Iino M, Kastanenka KV, Kettenmann H, Khakh BS, Koizumi S, Lee CJ, Liddelow SA, MacVicar BA, Magistretti P, Messing A, Mishra A, Molofsky AV, Murai KK, Norris CM, Okada S, Oliet SHR, Oliveira JF, Panatier A, Parpura V, Pekna M, Pekny M, Pellerin L, Perea G, Pérez-Nievas BG, Pfrieger FW, Poskanzer KE, Quintana FJ, Ransohoff RM, Riquelme-Perez M, Robel S, Rose CR, Rothstein JD, Rouach N, Rowitch DH, Semyanov A, Sirko S, Sontheimer H, Swanson RA, Vitorica J, Wanner IB, Wood LB, Wu J, Zheng B, Zimmer ER, Zorec R, Sofroniew MV, Verkhratsky A. Reactive astrocyte nomenclature, definitions, and future directions. Nat Neurosci. 2021 Mar;24(3):312-325. doi: 10.1038/s41593-020-00783-4. Epub 2021 Feb 15. PMID: 33589835.
13. Fetler L, Amigorena S. Neuroscience. Brain under surveillance: the microglia patrol. Science. 2005 Jul 15;309(5733):392-3. doi: 10.1126/science.1114852. PMID: 16020721.

14. Fritz G. RAGE: a single receptor fits multiple ligands. Trends Biochem Sci. 2011 Dec;36(12):625-32. doi: 10.1016/j.tibs.2011.08.008. Epub 2011 Oct 19. PMID: 22019011.
15. Gasparotto J, Ribeiro CT, Bortolin RC, Somensi N, Fernandes HS, Teixeira AA, Guasselli MOR, Agani CAJO, Souza NC, Grings M, Leipnitz G, Gomes HM, de Bittencourt Pasquali MA, Dunkley PR, Dickson PW, Moreira JCF, Gelain DP. Anti-RAGE antibody selectively blocks acute systemic inflammatory responses to LPS in serum, liver, CSF and striatum. Brain Behav Immun. 2017 May;62:124-136. doi: 10.1016/j.bbi.2017.01.008. Epub 2017 Jan 11. PMID: 28088642.
16. Glass CK, Saijo K, Winner B, Marchetto MC, Gage FH. Mechanisms underlying inflammation in neurodegeneration. Cell. 2010 Mar 19;140(6):918-34. doi: 10.1016/j.cell.2010.02.016
17. Hoogland IC, Houbolt C, van Westerloo DJ, van Gool WA, van de Beek D. Systemic inflammation and microglial activation: systematic review of animal experiments. J Neuroinflammation. 2015 Jun 6;12:114. doi: 10.1186/s12974-015-0332-6. PMID: 26048578; PMCID: PMC4470063.
18. Hutchison IC, Rathore S. The role of REM sleep theta activity in emotional memory. Front Psychol. 2015 Oct 1;6:1439. doi: 10.3389/fpsyg.2015.01439. PMID: 26483709; PMCID: PMC4589642.
19. Ingiosi AM, Raymond RM Jr, Pavlova MN, Opp MR. Selective contributions of neuronal and astroglial interleukin-1 receptor 1 to the regulation of sleep. Brain Behav Immun. 2015 Aug;48:244-57. doi: 10.1016/j.bbi.2015.03.014. Epub 2015 Apr 4. PMID: 25849975.

20. Irwin MR, Opp MR. Sleep Health: Reciprocal Regulation of Sleep and Innate Immunity. Neuropsychopharmacology. 2017 Jan;42(1):129-155. doi: 10.1038/npp.2016.148. Epub 2016 Aug 11. PMID: 27510422; PMCID: PMC5143488.
21. Janz R, Südhof TC, Hammer RE, Unni V, Siegelbaum SA, Bolshakov VY. Essential roles in synaptic plasticity for synaptogyrin I and synaptophysin I. Neuron. 1999 Nov;24(3):687-700. doi: 10.1016/s0896-6273(00)81122-8. PMID: 10595519.
22. Jing W, Wang Y, Fang G, Chen M, Xue M, Guo D, Yao D, Xia Y. EEG Bands of Wakeful Rest, Slow-Wave and Rapid-Eye-Movement Sleep at Different Brain Areas in Rats. Front Comput Neurosci. 2016 Aug 3;10:79. doi: 10.3389/fncom.2016.00079. PMID: 27536231; PMCID: PMC4971061.
23. Joshi R, Garabadu D, Teja GR, Krishnamurthy S. Silibinin ameliorates LPS-induced memory deficits in experimental animals. Neurobiol Learn Mem. 2014 Dec;116:117-31. doi: 10.1016/j.nlm.2014.09.006. Epub 2014 Oct 16. PMID: 25444719.
24. Kamps S, van den Heuvel OA, van der Werf YD, Berendse HW, Weintraub D, Vriend C. Smaller subcortical volume in Parkinson patients with rapid eye movement sleep behavior disorder. Brain Imaging Behav. 2019 Oct;13(5):1352-1360. doi: 10.1007/s11682-018-9939-4.
25. Kempuraj D, Thangavel R, Natteru PA, Selvakumar GP, Saeed D, Zahoor H, Zaheer S, Iyer SS, Zaheer A. Neuroinflammation Induces Neurodegeneration. J Neurol Neurosurg Spine. 2016;1(1):1003. Epub 2016 Nov 18. PMID: 28127589; PMCID: PMC5260818.

26. Kendall GS, Melbourne A, Johnson S, Price D, Bainbridge A, Gunny R, Huertas-Ceballos A, Cady EB, Ourselin S, Marlow N, Robertson NJ. White matter NAA/Cho and Cho/Cr ratios at MR spectroscopy are predictive of motor outcome in preterm infants. Radiology. 2014 Apr;271(1):230-8. doi: 10.1148/radiol.13122679. Epub 2013 Nov 21. PMID: 24475798.
27. Kierdorf K, Fritz G. RAGE regulation and signaling in inflammation and beyond. J Leukoc Biol. 2013 Jul;94(1):55-68. doi: 10.1189/jlb.1012519. Epub 2013 Mar 29. PMID: 23543766.
28. Kim JP, Lentz MR, Westmoreland SV, Greco JB, Ratai EM, Halpern E, Lackner AA, Masliah E, González RG. Relationships between astrogliosis and 1H MR spectroscopic measures of brain choline/creatine and myo-inositol/creatine in a primate model. AJNR Am J Neuroradiol. 2005 Apr;26(4):752-9. PMID: 15814917.
29. Krueger JM. The role of cytokines in sleep regulation. Curr Pharm Des. 2008;14(32):3408-16. doi: 10.2174/138161208786549281. PMID: 19075717; PMCID: PMC2692603.
30. Kubota T, Fang J, Kushikata T, Krueger JM. Interleukin-13 and transforming growth factor-1 inhibit spontaneous sleep in rabbits. Am J Physiol Regul Integr Comp Physiol 279: R786–R792, 2000. doi:10.1152/ajpregu.2000.279.3.R786.
31. Kumar D, Koyanagi I, Carrier-Ruiz A, Vergara P, Srinivasan S, Sugaya Y, Kasuya M, Yu TS, Vogt KE, Muratani M, Ohnishi T, Singh S, Teixeira CM, Chérasse Y, Naoi T, Wang SH, Nondhalee P, Osman BAH, Kaneko N, Sawamoto K, Kernie SG, Sakurai T, McHugh TJ, Kano M, Yanagisawa M, Sakaguchi M. Sparse Activity of Hippocampal Adult-Born Neurons during REM Sleep Is Necessary for Memory Consolidation. Neuron. 2020 Aug

5;107(3):552-565.e10. doi: 10.1016/j.neuron.2020.05.008. Epub 2020 Jun 4. PMID: 32502462.

32. Kuribayashi T. Elimination half-lives of interleukin-6 and cytokine-induced neutrophil chemoattractant-1 synthesized in response to inflammatory stimulation in rats. Lab Anim Res. 2018 Jun;34(2):80-83. doi: 10.5625/lar.2018.34.2.80.

33. Kushikata T, Fang J, Krueger JM. Interleukin-10 inhibits spontaneous sleep in rabbits. J Interferon Cytokine Res 19: 1025–1030, 1999. doi:10.1089/107999099313244. 3

34. Kushikata T, Fang J, Wang Y, Krueger JM. Interleukin-4 inhibits spontaneous sleep in rabbits. Am J Physiol Regul Integr Comp Physiol 275: R1185–R1191, 1998

35. Kwon HS, Koh SH. Neuroinflammation in neurodegenerative disorders: the roles of microglia and astrocytes. Transl Neurodegener. 2020 Nov 26;9(1):42. doi: 10.1186/s40035-020-00221-2. PMID: 33239064; PMCID: PMC7689983.

36. Lee ML, Katsuyama ÂM, Duge LS, Sriram C, Krushelnytskyy M, Kim JJ, de la Iglesia HO. Fragmentation of Rapid Eye Movement and Nonrapid Eye Movement Sleep without Total Sleep Loss Impairs Hippocampus-Dependent Fear Memory Consolidation. Sleep. 2016 Nov 1;39(11):2021-2031. doi: 10.5665/sleep.6236. PMID: 27568801; PMCID: PMC5070756.

37. Leelahavanichkul A, Huang Y, Hu X, Zhou H, Tsuji T, Chen R, Kopp JB, Schnermann J, Yuen PS, Star RA. Chronic kidney disease worsens sepsis and sepsis-induced acute kidney injury by releasing High Mobility Group Box Protein-1. Kidney Int. 2011 Dec;80(11):1198-211. doi: 10.1038/ki.2011.261.

38. Leung LS. Theta rhythm during REM sleep and waking: correlations between power, phase and frequency. Electroencephalogr Clin Neurophysiol. 1984 Dec;58(6):553-64. doi: 10.1016/0013-4694(84)90045-2. PMID: 6209105.
39. Levenstein D, Buzsáki G, Rinzel J. NREM sleep in the rodent neocortex and hippocampus reflects excitable dynamics. Nat Commun. 2019 Jun 6;10(1):2478. doi: 10.1038/s41467-019-10327-5. PMID: 31171779; PMCID: PMC6554409.
40. Liao H, Bu WY, Wang TH, Ahmed S, Xiao ZC. Tenascin-R plays a role in neuroprotection via its distinct domains that coordinate to modulate the microglia function. J Biol Chem. 2005 Mar 4;280(9):8316-23. doi: 10.1074/jbc.M412730200. Epub 2004 Dec 22. PMID: 15615725.
41. Li W, Liu L, Liu YY, Luo J, Lin JY, Li X, Wang B, Min S. Effects of electroconvulsive stimulation on long-term potentiation and synaptophysin in the hippocampus of rats with depressive behavior. J ECT. 2012 Jun;28(2):111-7. doi: 10.1097/YCT.0b013e31824a47ca. PMID: 22531204.
42. Lopes-Aguiar C, Ruggiero RN, Rossignoli MT, Esteves IM, Peixoto-Santos JE, Romcy-Pereira RN, Leite JP. Long-term potentiation prevents ketamine-induced aberrant neurophysiological dynamics in the hippocampus-prefrontal cortex pathway in vivo. Sci Rep. 2020 Apr 28;10(1):7167. doi: 10.1038/s41598-020-63979-5. PMID: 32346044; PMCID: PMC7188848.
43. Lu YC, Yeh WC, Ohashi PS. LPS/TLR4 signal transduction pathway. Cytokine. 2008 May;42(2):145-151. doi: 10.1016/j.cyto.2008.01.006. Epub 2008 Mar 4. PMID: 18304834.

44. Lynch MA. Long-term potentiation and memory. Physiol Rev. 2004 Jan;84(1):87-136. doi: 10.1152/physrev.00014.2003. PMID: 14715912.
45. Mader I, Rauer S, Gall P, Klose U. (1)H MR spectroscopy of inflammation, infection and ischemia of the brain. Eur J Radiol. 2008 Aug;67(2):250-7. doi: 10.1016/j.ejrad.2008.02.033. Epub 2008 Apr 14. PMID: 18407447.
46. Malhotra RK. Neurodegenerative Disorders and Sleep. Sleep Med Clin. 2018 Mar;13(1):63-70. doi: 10.1016/j.jsmc.2017.09.006.
47. Mamad O, Islam MN, Cunningham C, Tsanov M. Differential response of hippocampal and prefrontal oscillations to systemic LPS application. Brain Res. 2018 Feb 15;1681:64-74. doi: 10.1016/j.brainres.2017.12.036. Epub 2017 Dec 30. PMID: 29294350; PMCID: PMC5792247.
48. Nachón-García F, Hurtado-Alvarado G, Acosta-Hernández ME, Peña-Escudero C, Priego-Fernández S, Alvarez-Herrera S, Becerril-Villanueva E, Pérez-Sánchez G, Pavón L, García-García F. Characterization of sleep-pattern and neuro-immune-endocrine markers at 24 hour post-injection of a single low dose of lipopolysaccharide in male Wistar rats. J Neuroimmunol. 2018 Jul 15;320:15-18. doi: 10.1016/j.jneuroim.2018.04.011. Epub 2018 Apr 17. PMID: 29759136.
49. Nimmerjahn A, Kirchhoff F, Helmchen F. Resting microglial cells are highly dynamic surveillants of brain parenchyma in vivo. Science. 2005 May 27;308(5726):1314-8. doi: 10.1126/science.1110647. Epub 2005 Apr 14. PMID: 15831717.
50. Opal SM. Endotoxins and other sepsis triggers. Contrib Nephrol. 2010;167:14-24. doi: 10.1159/000315915. Epub 2010 Jun 1. PMID: 20519895.

51. Park JS, Davis RL, Sue CM. Mitochondrial Dysfunction in Parkinson's Disease: New Mechanistic Insights and Therapeutic Perspectives. Curr Neurol Neurosci Rep. 2018 Apr 3;18(5):21. doi: 10.1007/s11910-018-0829-3. PMID: 29616350; PMCID: PMC5882770.
52. Perez-Dominguez M, Ávila-Muñoz E, Domínguez-Rivas E, Zepeda A. The detrimental effects of lipopolysaccharide-induced neuroinflammation on adult hippocampal neurogenesis depend on the duration of the pro-inflammatory response. Neural Regen Res. 2019 May;14(5):817-825. doi: 10.4103/1673-5374.249229. PMID: 30688267; PMCID: PMC6375041.
53. Pesonen AK, Gradisar M, Kuula L, Short M, Merikanto I, Tark R, Räikkönen K, Lahti J. REM sleep fragmentation associated with depressive symptoms and genetic risk for depression in a community-based sample of adolescents. J Affect Disord. 2019 Feb 15;245:757-763. doi: 10.1016/j.jad.2018.11.077. Epub 2018 Nov 13. PMID: 30448760.
54. Qin L, Wu X, Block ML, Liu Y, Breese GR, Hong JS, Knapp DJ, Crews FT. Systemic LPS causes chronic neuroinflammation and progressive neurodegeneration. Glia. 2007 Apr 1;55(5):453-62.
55. Ransohoff RM. How neuroinflammation contributes to neurodegeneration. Science. 2016 Aug 19;353(6301):777-83. doi: 10.1126/science.aag2590. PMID: 27540165.
56. Regensburger M, Prots I, Winner B. Adult hippocampal neurogenesis in Parkinson's disease: impact on neuronal survival and plasticity. Neural Plast. 2014;2014:454696. doi: 10.1155/2014/454696. Epub 2014 Jul 3. PMID: 25110593; PMCID: PMC4106176.

57. Reijnders JS, Ehrt U, Weber WE, Aarsland D, Leentjens AF. A systematic review of prevalence studies of depression in Parkinson's disease. Mov Disord. 2008 Jan 30;23(2):183-9; quiz 313. doi: 10.1002/mds.21803. PMID: 17987654.
58. Russo MV, McGavern DB. Inflammatory neuroprotection following traumatic brain injury. Science. 2016 Aug 19;353(6301):783-5. doi: 10.1126/science.aaf6260. PMID: 27540166; PMCID: PMC5260471.
59. Schapira AHV, Chaudhuri KR, Jenner P. Non-motor features of Parkinson disease. Nat Rev Neurosci. 2017 Jul;18(7):435-450. doi: 10.1038/nrn.2017.62.
60. Sheline YI. Depression and the hippocampus: cause or effect? Biol Psychiatry. 2011 Aug 15;70(4):308-9. doi: 10.1016/j.biopsych.2011.06.006. PMID: 21791257; PMCID: PMC3733566.
61. Simard AR, Soulet D, Gowing G, Julien JP, Rivest S. Bone marrow-derived microglia play a critical role in restricting senile plaque formation in Alzheimer's disease. Neuron. 2006 Feb 16;49(4):489-502. doi: 10.1016/j.neuron.2006.01.022. PMID: 16476660.
62. Stefanis L. α-Synuclein in Parkinson's disease. Cold Spring Harb Perspect Med. 2012 Feb;2(2):a009399. doi: 10.1101/cshperspect.a009399. PMID: 22355802; PMCID: PMC3281589.
63. Streit WJ. Microglia as neuroprotective, immunocompetent cells of the CNS. Glia. 2002 Nov;40(2):133-9. doi: 10.1002/glia.10154. PMID: 12379901.
64. Suzuki K, Okuma Y, Uchiyama T, Miyamoto M, Sakakibara R, Shimo Y, Hattori N, Kuwabara S, Yamamoto T, Kaji Y, Hirano S, Kadowaki T, Hirata K; Kanto NMPD investigators. Impact of sleep-related symptoms on clinical motor subtypes and disability in Parkinson's disease: a multicentre cross-sectional

study. J Neurol Neurosurg Psychiatry. 2017 Nov;88(11):953-959. doi: 10.1136/jnnp-2017-316136. Epub 2017 Aug 28. PMID: 28847794; PMCID: PMC5740547.

65. Tanaka N, Yonekura H, Yamagishi S, Fujimori H, Yamamoto Y, Yamamoto H. The receptor for advanced glycation end products is induced by the glycation products themselves and tumor necrosis factor-alpha through nuclear factor-kappa B, and by 17beta-estradiol through Sp-1 in human vascular endothelial cells. J Biol Chem. 2000 Aug 18;275(33):25781-90. doi: 10.1074/jbc.M001235200. PMID: 10829018.
66. Tieu K. A guide to neurotoxic animal models of Parkinson's disease. Cold Spring Harb Perspect Med. 2011 Sep;1(1):a009316. doi: 10.1101/cshperspect.a009316. PMID: 22229125; PMCID: PMC3234449.
67. Towner RA, Saunders D, Smith N, Towler W, Cruz M, Do S, Maher JE, Whitaker K, Lerner M, Morton KA. Assessing long-term neuroinflammatory responses to encephalopathy using MRI approaches in a rat endotoxemia model. Geroscience. 2018 Feb;40(1):49-60. doi: 10.1007/s11357-018-0009-z.
68. Town T, Nikolic V, Tan J. The microglial "activation" continuum: from innate to adaptive responses. J Neuroinflammation. 2005 Oct 31;2:24. doi: 10.1186/1742-2094-2-24. PMID: 16259628; PMCID: PMC1298325.
69. Wyss-Coray T, Mucke L. Inflammation in neurodegenerative disease--a double-edged sword. Neuron. 2002 Aug 1;35(3):419-32. doi: 10.1016/s0896-6273(02)00794-8. PMID: 12165466.
70. Zhao, J., Bi, W., Xiao, S. *et al.* Neuroinflammation induced by lipopolysaccharide causes cognitive impairment in mice. *Sci Rep* 9, 5790 (2019). https://doi.org/10.1038/s41598-019-42286-8

9. Figure Legends

Figure 1: Systemic levels of cytokines remain unaltered. Levels of proinflammatory cytokines IL1b (A), IL6 (B) and TNFa (D), and antiinflammatory IL10 were (C) assessed through ELISA. There were no significant alterations in cytokine levels either 3 or 5 months after systemic LPS exposure. Results are presented as a percentage of control. Each symbol represents one animal (**A, B,C**: Control 3mo n= 8; Control 5mo n= 8; LPS 3mo n= 8; LPS 5mo n= 8) (**D:** Control 3mo n= 6; Control 5mo n= 6; LPS 3mo n= 6; LPS 5mo n= 6). Values represent median ± interquartile range. Kruskal-Wallis test followed by Dunn's *post hoc* test.

Figure 2: Elevated levels of inflammation related proteins in the hippocampus. Microglial marker Iba1 (A), pattern recognition receptor RAGE (D) and p65 (NF-kB) phosphorylation (E) elevated levels were observed 3 months after LPS injection. There were no significant alterations of astrocyte markers GFAP (B) and S100b (C). Each symbol represents one animal (Control 3mo n= 6; Control 5mo n= 6; LPS 3mo n= 6; LPS 5mo n= 6). Values represent median ± interquartile range. Kruskal-Wallis test followed by Dunn's *post hoc* test. (* p<0,05, ** p<0,01, *** p<0,001).

Figure 3: Inflammation-related gene expression is altered in LPS treated animals. Elevated expression of proinflammatory cytokines TNFa (A) and IL1b (B) was elevated 3 (Control n= 7; LPS n= 7) months after LPS exposure. RAGE (C) expression was elevated both 3 and 5 (Control n= 7; LPS n= 7) months post-injection. There were no significant changes in INFg expression. Each symbol

represents one animal. Values represent median ± interquartile range. Kruskal-Wallis test followed by Dunn's *post hoc* test (* p<0,05).

Figure 4: Altered neuronal and synaptic markers in the hippocampus of LPS treated animals. LPS treatment leads to reduction of the levels of NeuN (A), NEFL (B) and Synaptophysin (D) 5 months (Control n= 6; LPS n= 6) post-injection. PSD95 (C) levels remained unaltered. No alterations were observed 3 months after LPS exposure (Control n= 6; LPS n= 6). Each symbol represents one animal. Values represent median ± interquartile range. Kruskal-Wallis test followed by Dunn's *post hoc* test (* p<0.05 ** p<0.005).

Figure 5: Sleep architecture analysis. Percentage of epochs in each brain state remained unaltered 3 months (Control n= 5; LPS n= 5) (A) and (B) 5 months (Control n= 5; LPS n= 5) post-injection. (E) REM sleep episode duration significantly decreased 3 months after treatment; (C) WK and (D) NREM remained unaltered. No differences were observed after 5 months post-injection. (F) represents peak Delta frequency during NREM and (G) represents peak Theta frequency during REM sleep. LPS treatment was not capable of altering peak delta and theta frequencies. Each symbol represents one animal. Values represent median ± interquartile range. Kruskal-Wallis test followed by Dunn's *post hoc* test (* p=0,0403).

Figure 6: REM sleep theta power is reduced in LPS-treated animals 3 months post-injection. Theta (A), Beta (B) and Gamma (C) power remained unaltered during NREM, 3 (Control n= 5; LPS n= 5) and 5 (Control n= 5; LPS n= 5) months post-injection. Delta (E) and Gamma (F) power remained unaltered during REM

sleep, 3 and 5 months after LPS exposure. Theta power significantly decreased during REM sleep 3 months after LPS treatment (D) and after 5 months returned to control levels. Each symbol represents one animal. Values represent median ± interquartile range. Kruskal-Wallis test followed by Dunn's *post hoc* test (** p=0,0277).

Supplementary Figure 1: (A) Experimental design. (B) Survival rate to different LPS doses. (C) HE staining for electrode localization. (D) Baseline recordings of hippocampal LFP (blue line) and neck EMG (redline) during Wakefulness (WK), NREM and REM sleep.

Supplementary Figure 2: (A) and (C) average of power spectral decomposition during REM sleep and NREM, 3 and 5 months after LPS injection respectively. (B) and (D) normalized power of Theta, Delta, Low Gamma, High Gamma, total Gamma during REM and NREM, 3 and 5 months after LPS exposure. Each graph represents one animal. (E) Comparison between hippocampal electrodes placed in the left and right hemispheres of 3 control animals. Bars represent median + range. Kruskal-Wallis test followed by Dunn's *post hoc* test.

Supplementary Table 1: Primary antibodies employed either in Western Blot or ELISA experiments.

Supplementary Table 2: Primers used in RT-qPCR experiments.

Figures

Graphical Abstract

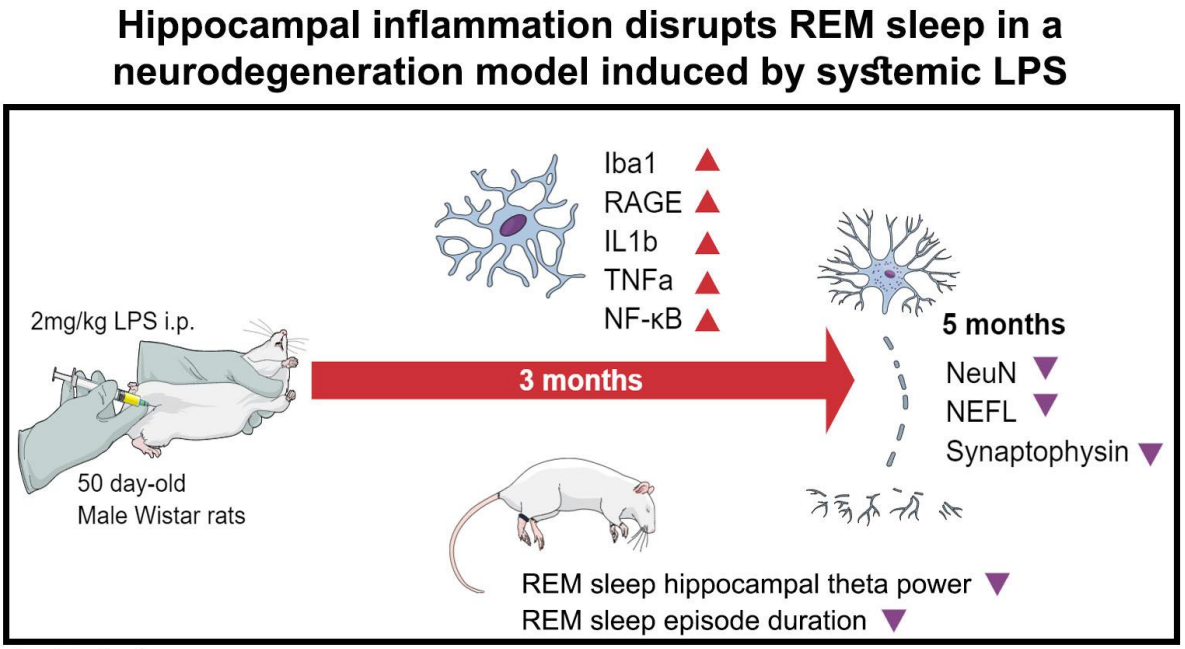

In Brief:

Systemic LPS induces hippocampal inflammation in Wistar rats. A temporal correlation between elevated levels of inflammatory mediators, shorter episodes of REM sleep, and reduction of hippocampal REM sleep theta power are observed. Remission of neuroinflammatory parameters is accompanied by diminished immunocontent of neuronal and synaptic markers.

Figure 1

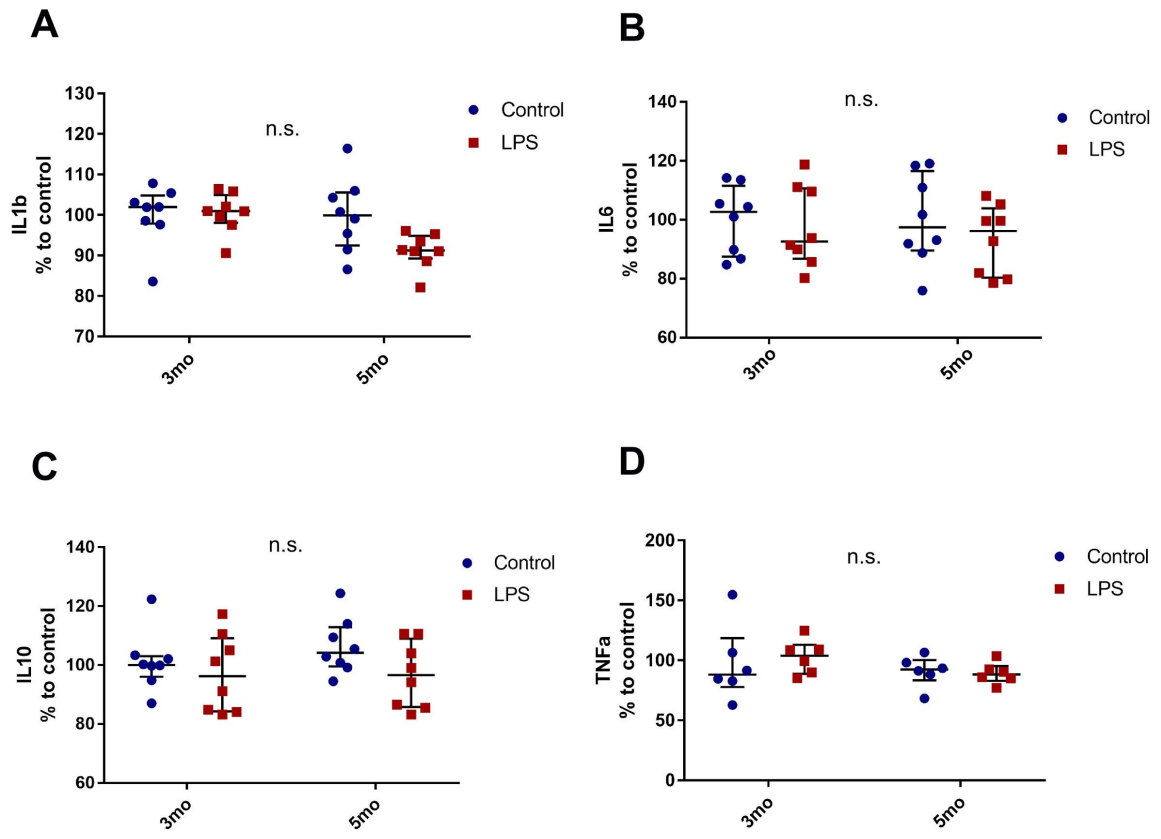
A
B
C
D
n.s.
Control
LPS
IL1b
% to control
IL6
% to control
IL10
% to control
TNFa
% to control
3mo
5mo

Figure 2

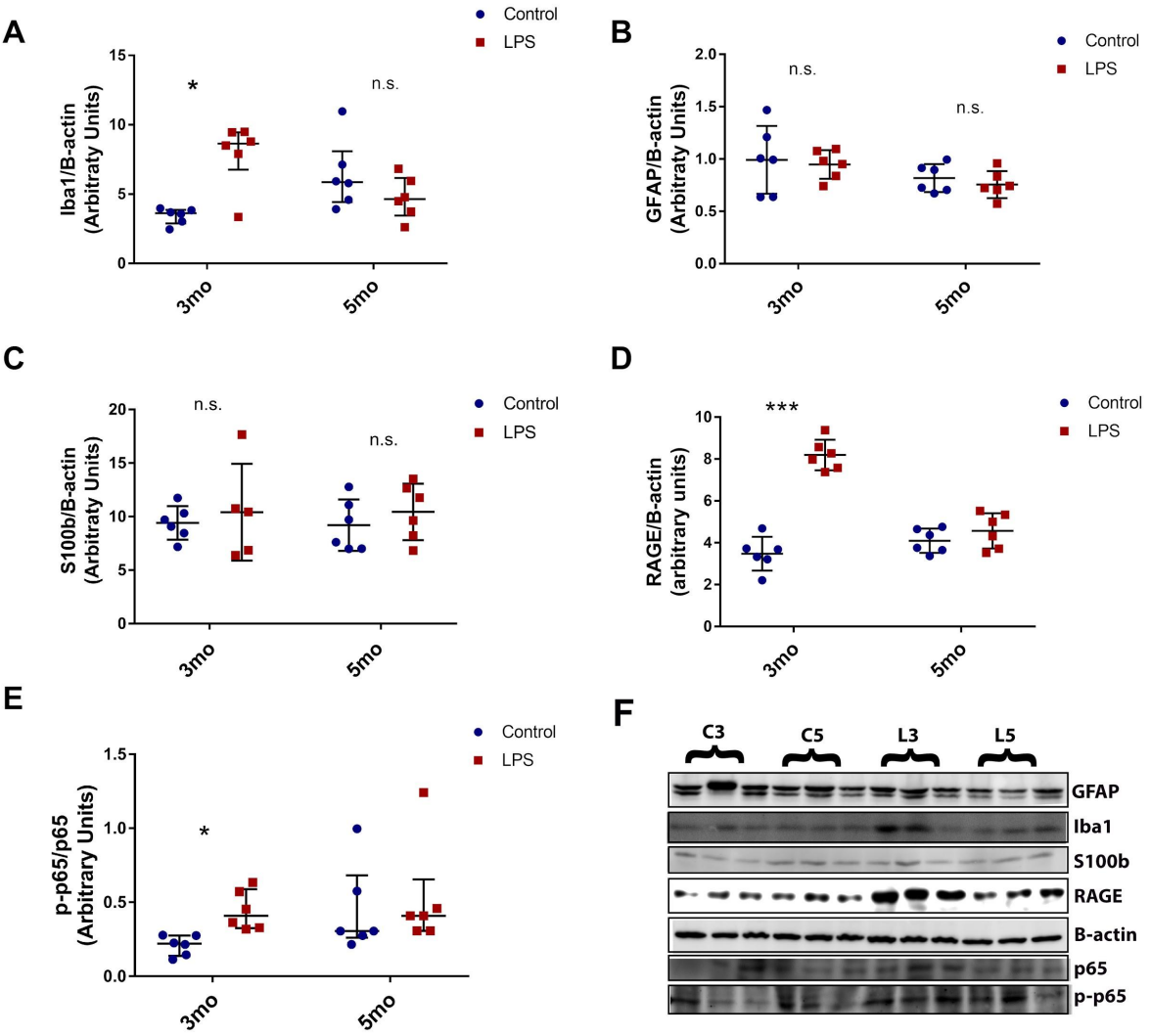
A
Control
LPS
Iba1/B-actin (Arbitraty Units)
*
n.s.
3mo
5mo
B
Control
LPS
GFAP/B-actin (Arbitraty Units)
n.s.
n.s.
3mo
5mo
C
Control
LPS
S100b/B-actin (Arbitraty Units)
n.s.
n.s.
3mo
5mo
D
Control
LPS
RAGE/B-actin (arbitrary units)
***
3mo
5mo
E
Control
LPS
p-p65/p65 (Arbitrary Units)
*
3mo
5mo
F
C3
C5
L3
L5
GFAP
Iba1
S100b
RAGE
B-actin
p65
p-p65

Figure 3

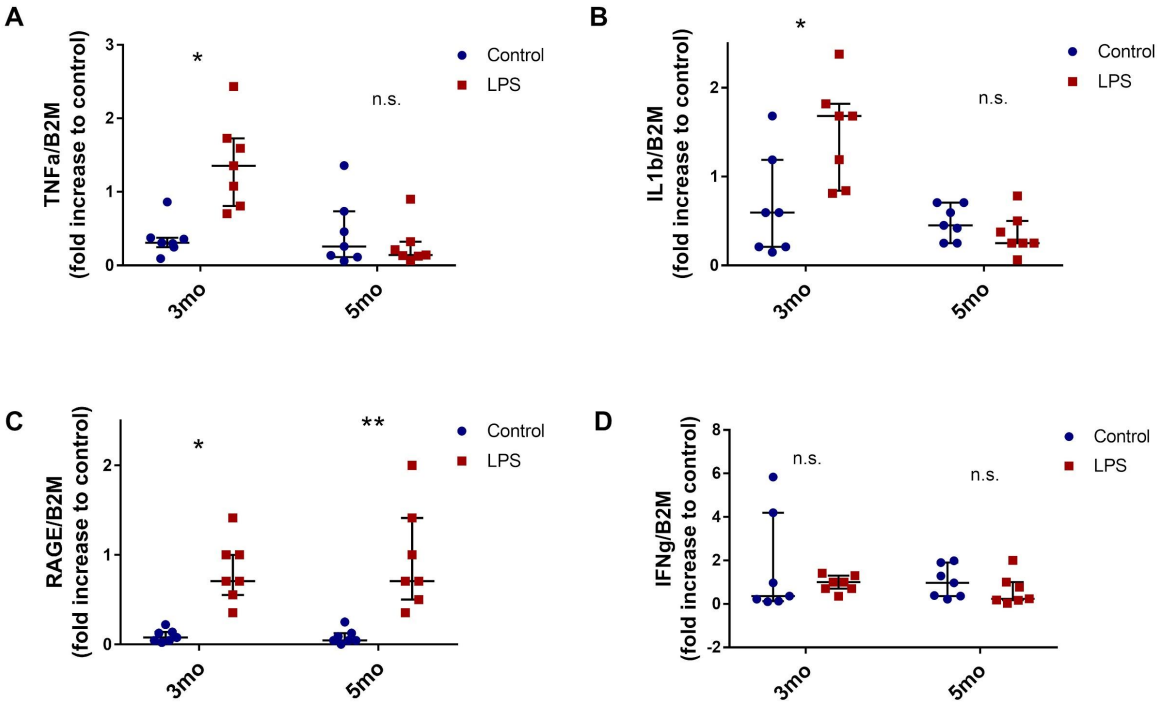
A
TNFa/B2M
(fold increase to control)
*
n.s.
Control
LPS
3mo
5mo
B
IL1b/B2M
(fold increase to control)
*
n.s.
Control
LPS
3mo
5mo
C
RAGE/B2M
(fold increase to control)
*
**
Control
LPS
3mo
5mo
D
IFNg/B2M
(fold increase to control)
n.s.
n.s.
Control
LPS
3mo
5mo

Figure 4

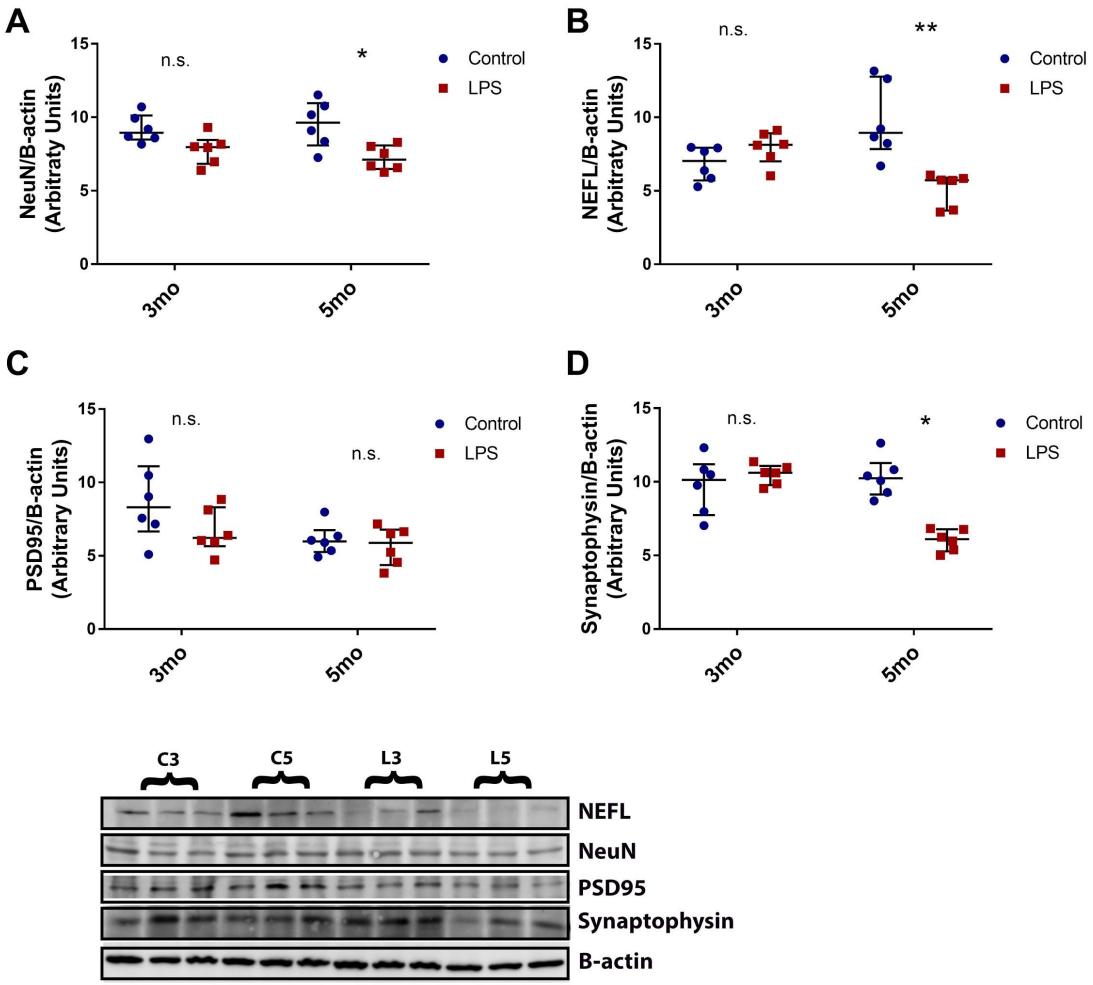
A
B
C
D
NeuN/B-actin (Arbitraty Units)
NEFL/B-actin (Arbitraty Units)
PSD95/B-actin (Arbitrary Units)
Synaptophysin/B-actin (Arbitrary Units)
n.s.
*
**
Control
LPS
3mo
5mo
C3
C5
L3
L5
NEFL
NeuN
PSD95
Synaptophysin
B-actin

Figure 5

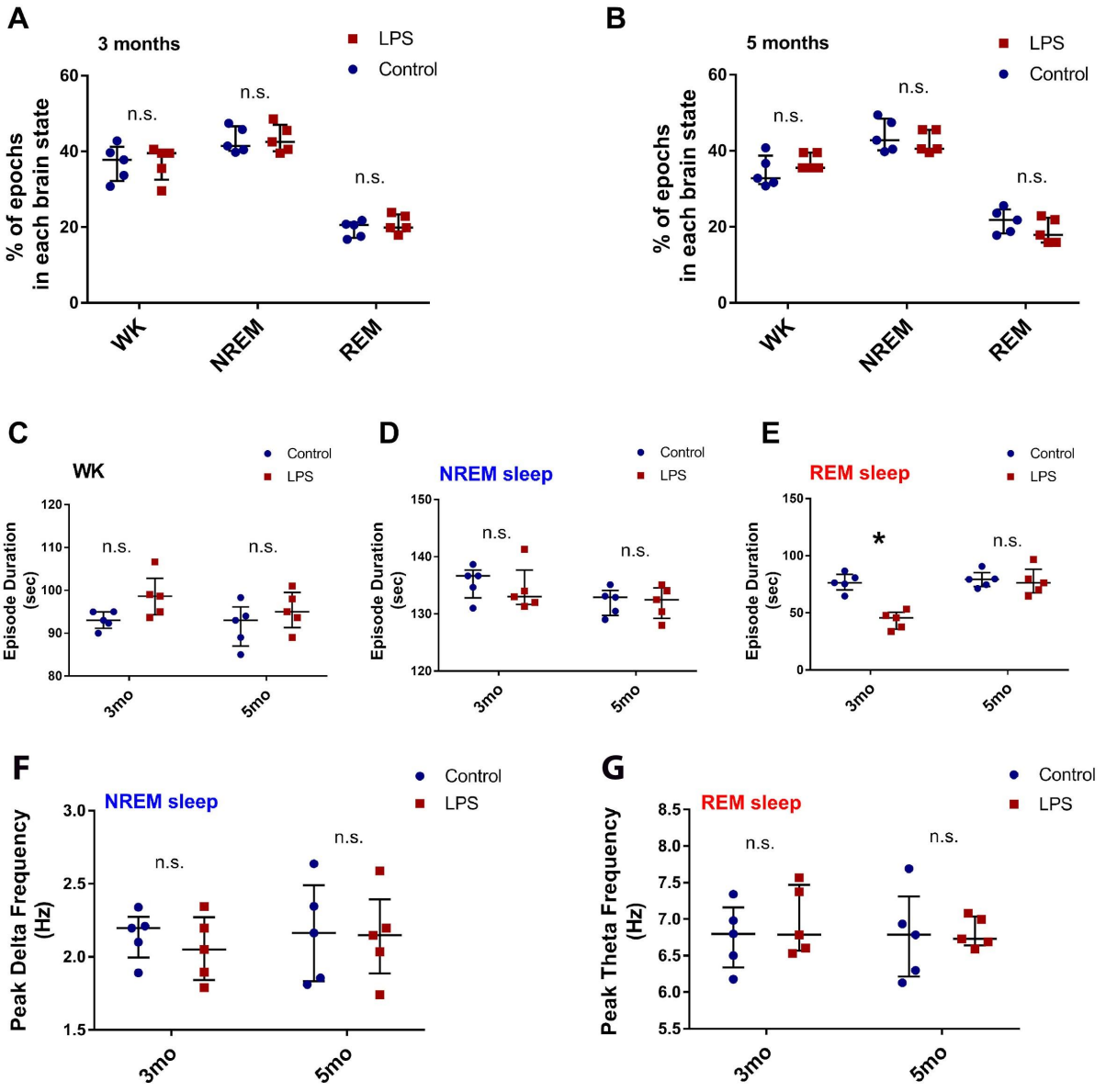
A
3 months
LPS
Control
% of epochs in each brain state
n.s.
n.s.
n.s.
WK
NREM
REM
B
5 months
LPS
Control
% of epochs in each brain state
n.s.
n.s.
n.s.
WK
NREM
REM
C
WK
Control
LPS
Episode Duration (sec)
n.s.
n.s.
3mo
5mo
D
NREM sleep
Control
LPS
Episode Duration (sec)
n.s.
n.s.
3mo
5mo
E
REM sleep
Control
LPS
Episode Duration (sec)
*
n.s.
3mo
5mo
F
NREM sleep
Control
LPS
Peak Delta Frequency (Hz)
n.s.
n.s.
3mo
5mo
G
REM sleep
Control
LPS
Peak Theta Frequency (Hz)
n.s.
n.s.
3mo
5mo

Figure 6

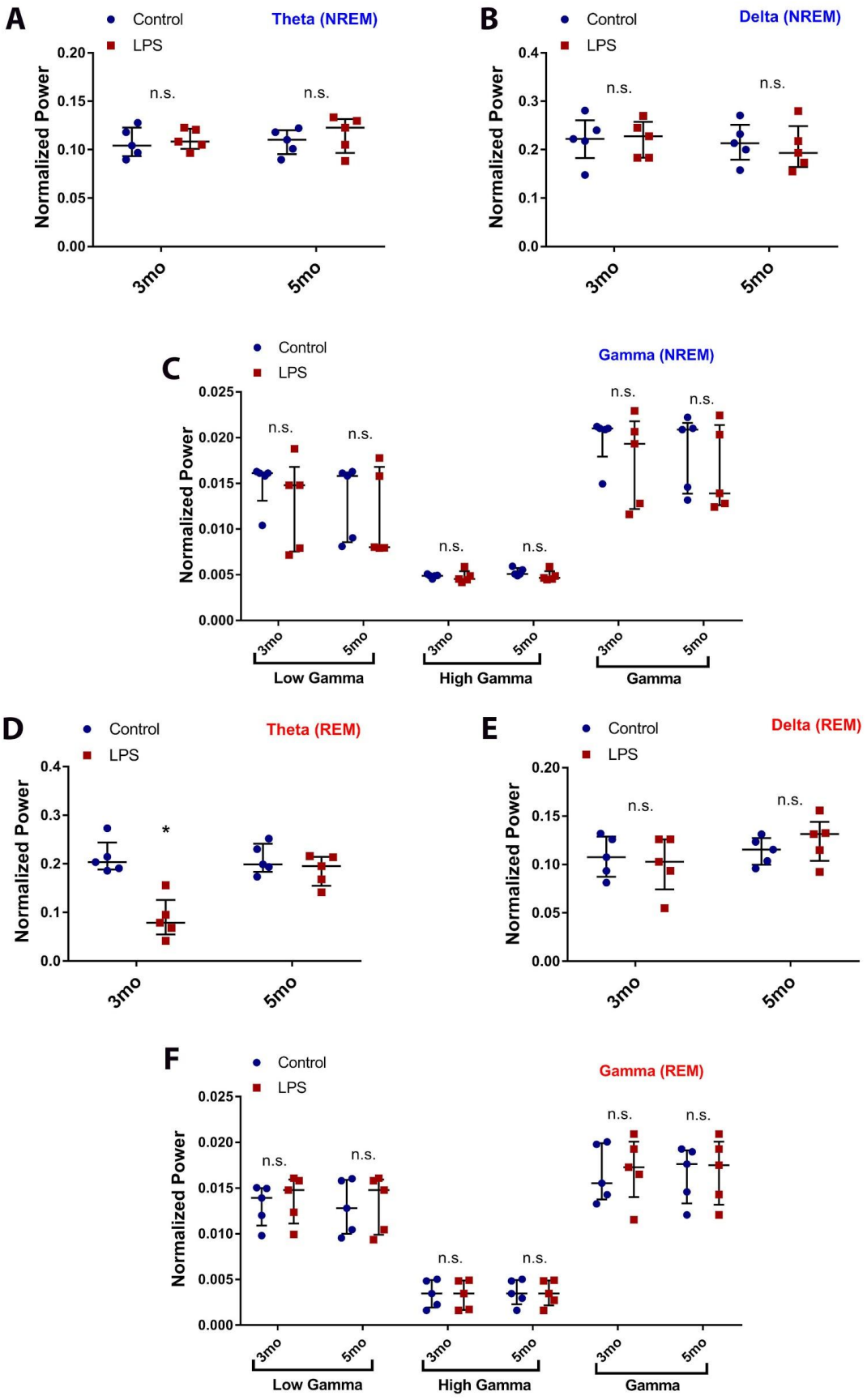
A
Control
LPS
Theta (NREM)
Normalized Power
0.20
0.15
0.10
0.05
0.00
n.s.
n.s.
3mo
5mo
B
Control
LPS
Delta (NREM)
Normalized Power
0.4
0.3
0.2
0.1
0.0
n.s.
n.s.
3mo
5mo
C
Control
LPS
Gamma (NREM)
Normalized Power
0.025
0.020
0.015
0.010
0.005
0.000
n.s.
n.s.
n.s.
n.s.
n.s.
n.s.
3mo
5mo
Low Gamma
High Gamma
Gamma
D
Control
LPS
Theta (REM)
Normalized Power
0.4
0.3
0.2
0.1
0.0
*
3mo
5mo
E
Control
LPS
Delta (REM)
Normalized Power
0.20
0.15
0.10
0.05
0.00
n.s.
n.s.
3mo
5mo
F
Control
LPS
Gamma (REM)
Normalized Power
0.025
0.020
0.015
0.010
0.005
0.000
n.s.
n.s.
n.s.
n.s.
n.s.
n.s.
3mo
5mo
Low Gamma
High Gamma
Gamma

Supplementary Figure 1

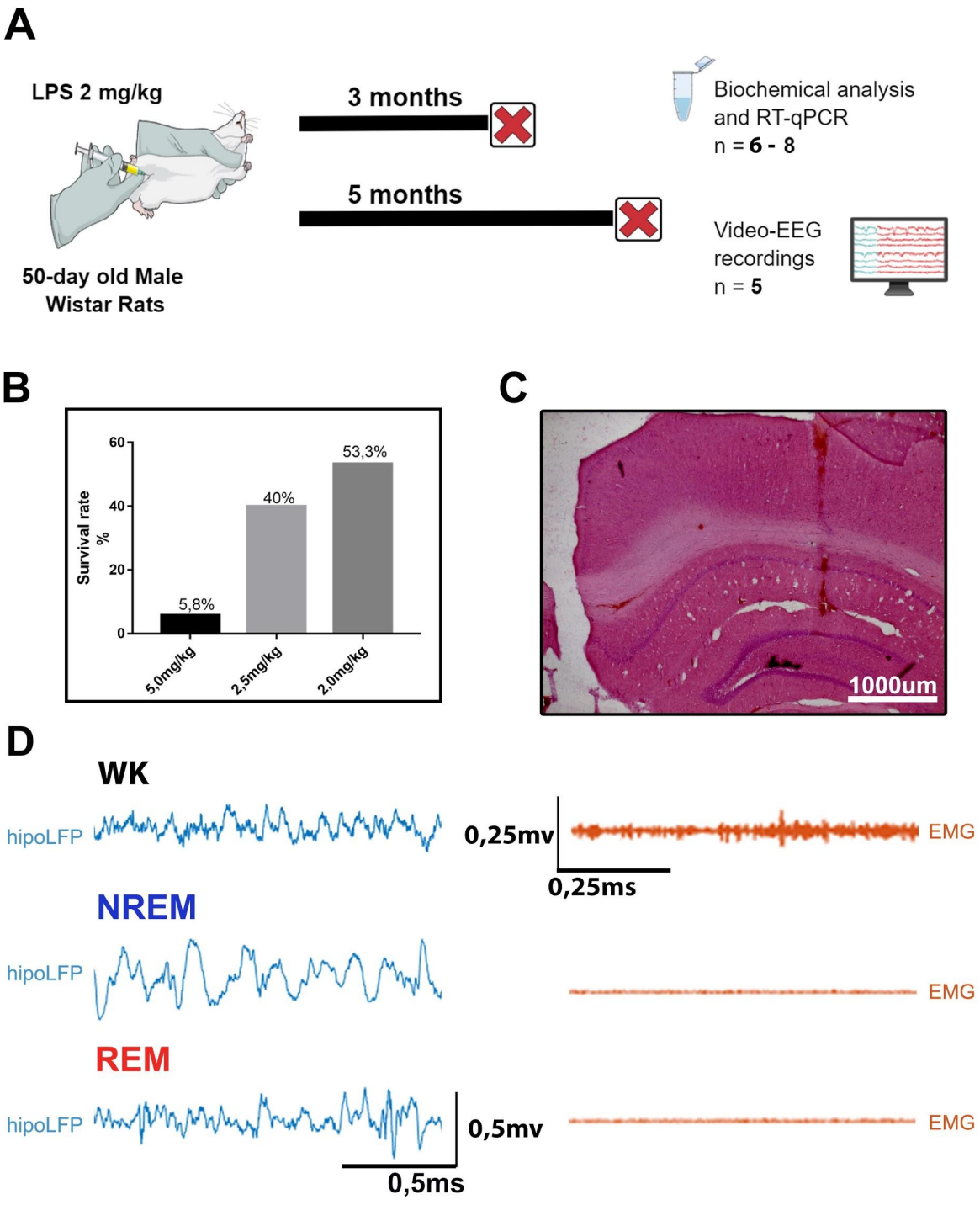

Supplementary Figure 2

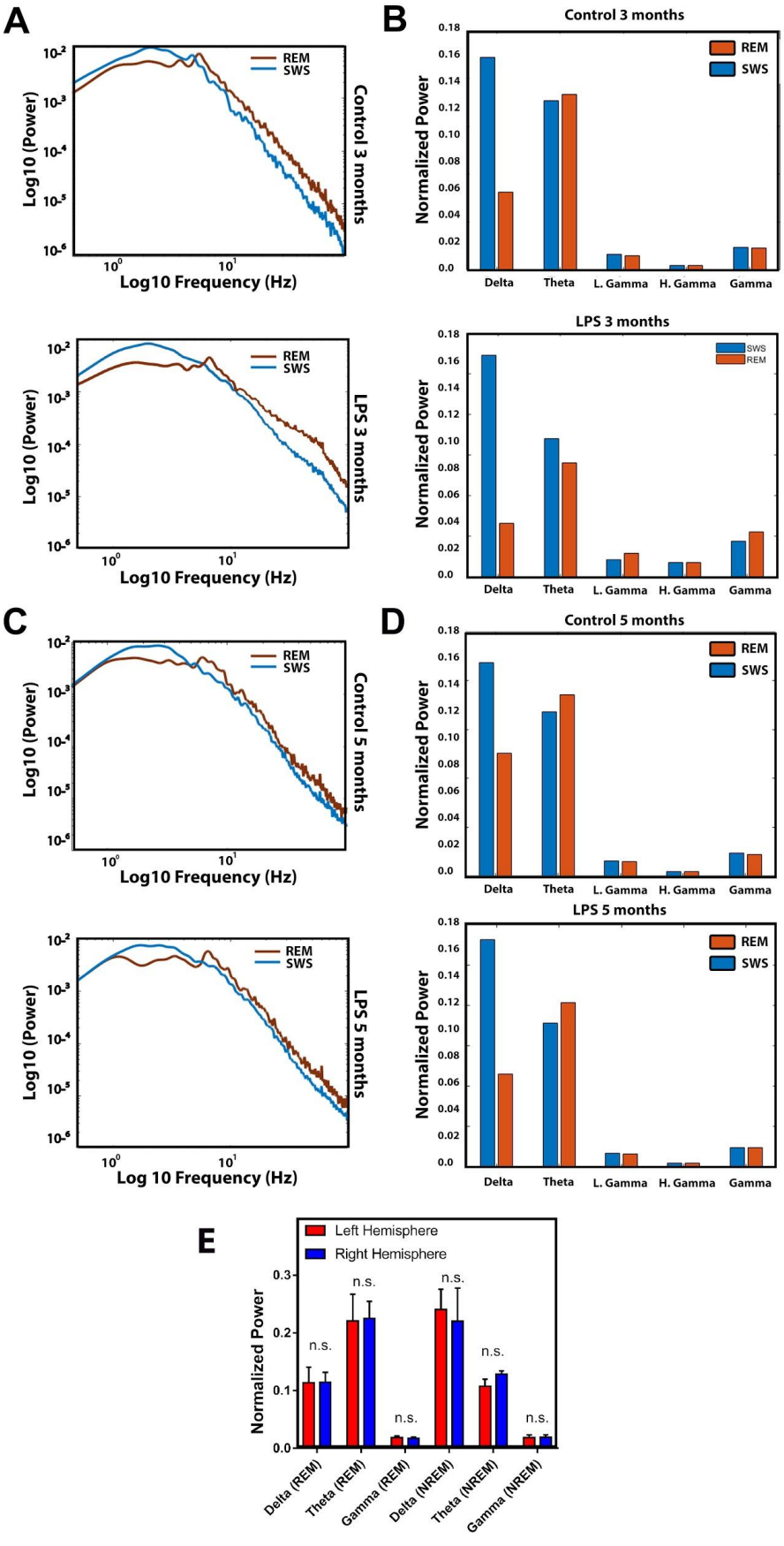

Supplementary Table 1

Target	Reference	Manufacturer
B-actin	MA5-15739	Thermo Fischer
GFAP	G4546	Sigma-Aldrich
Iba1	SAB2500041	Sigma-Aldrich
IL1b	9722	Abcam
IL6	6672	Abcam
IL10	9969	Abcam
NEFL	C28E10	Cell Signaling Technology
NeuN	D3531	Cell Signaling Technology
PSD95	36233	Cell Signaling Technology
RAGE	H300	Santa Cruz Biotechnology
S100b	D1OG6	Cell Signaling Technology
Synaptophysin	43295	Cell Signaling Technology

Supplementary Table 2

Target	Forward	Reverse
B2M	*TGCTGTCTCCATGTTTGAT*	*TCTCCGCTCCCCACCTCTA*
GNB2L	*GAGTGTGGCCTTCTCCTCTG*	*GCTTGCAGTTAGCCAGGTTC*
IFNg	*CAGGCCATCAGCAACAACATAA*	*GAACTTGGCGATGCTCATGAAT*
IL1b	*ACCTGTTCTTTGAGGCTGAC*	*AATGAGTGACACTGCCTTCC*
RAGE	*CTGACCTGTGCCATCTCTG*	*TCATCCTCATGCCCTACCT*
TNFa	*CAGACCCTCACACTCAGATCAT*	*ACCACCAGTTGGTTGTCTTTG*

Parte III

Discussão

Os resultados aqui apresentados demonstram uma relação temporal entre o aumento de parâmetros pró-inflamatórios no hipocampo (níveis elevados do marcador microglial Iba1, do receptor de padrões moleculares RAGE, atividade de NF-kB e expressão aumentada de citocinas pró-inflamatórias (IL1b e TNFa) e uma redução no poder de Theta durante o sono REM, acompanhada por intervalos mais curtos desde estado do sono. Esta relação foi observada somente 3 meses após o tratamento com LPS, após 5 meses parâmetros inflamatórios e de sono retornaram aos níveis de controle, no entanto, foi possível observar a redução dos níveis de marcadores neuronais (NEFL e NeuN) e sinápticos (Sinaptofisina). Estes resultados indicam que uma injeção sistêmica de LPS pode induzir uma neuroinflamação crônica, alterações no sono REM e degeneração hipocampal.

1. LPS sistêmico induz neuroinflamação hipocampal

A administração de LPS sistêmico é um modelo utilizado por diversos autores para induzir um estado do tipo séptico em modelos animais através da endotoxemia (Buras et al., 2005, Opal et al., 2010). Uma injeção intraperitoneal de LPS (5mg/kg) leva ao aumento dos níveis da citocina pró-inflamatória TNFa no soro de camundongos C57BL/6J nas primeiras horas após o estímulo inflamatório (Qin et al., 2007, Gasparotto et al., 2017). Apesar de estes níveis no soro retornarem ao basal dentro das primeiras 24h após o tratamento, este insulto leva a dano na barreira hemato-encefálica permitindo a infiltração de mediadores inflamatórios no fluido cerebroespinhal (Gasparotto et al., 2017, Towner et al., 2018). A presença destas

moléculas no cérebro leva ativação microglial e por consequência o aumento da expressão e conteúdo de citocinas pró-inflamatórias no Sistema Nervoso Central colaborando para a manutenção de um estado inflamatório no cérebro (Hoggland et al., 2015). Soma-se a isso o fato de o receptor de reconhecimento de padrões moleculares RAGE mudar o seu sítio de expressão, de células vasculares endoteliais para neurônios (Gasparotto et al., 2019), a ativação deste receptor por mediadores inflamatórios permite a perpetuação deste estado de inflamação através da ativação de NF-kB, culminando no aumento da expressão de citocinas e do próprio RAGE.

Trabalhos anteriores demonstraram os efeitos da administração de LPS sistêmico em diferentes estruturas cerebrais e ressaltam a diferença da resposta neuro-inflamatória entre regiões distintas (Qin et al., 2007, Towner et al., 2018, Zhao et al., 2019). Qin e colaboradores demonstraram um aumento nos marcadores microgliais e níveis elevados da citocina pró-inflamatória TNFa na substância negra de camundongos C57BL/6J 10 meses após o tratamento com LPS (Qin et al., 2007). Towner e colaboradores investigaram a razão entre os metabólitos N-acetil aspartato e colina (NAA/Cho), entre Creatina e Cho (Cr/Cho) e entre Myo-Inositol/Cho (Myo-Ins/Cho) através de técnicas de imagem por MRI. Foi observada uma redução nas razões NAA/Cho e Cr/Cho, tal redução é indicativa de astrogliose, neuroinflamação e degeneração axonal (Kendall et al., 2014, Mader et al., 2008, Kim et al., 2005). Apesar da inflamação hipocampal ser persistente por pelo menos 3 meses, alguns resultados indicam que a neuroinflamação nesta estrutura não se mantém por tanto tempo quanto na substância negra. A razão de Myo-Ins/Cho hipocampal, danos a barreira hemato-encefálica e o fluxo sanguíneo relativo retornam a níveis de controle em 3 meses, enquanto a produção de radicais livres

retorna a níveis basais em apenas uma semana (Towner et al., 2018). Os resultados obtidos aqui suportam a ideia de que a inflamação hipocampal começa a decair 3 meses após o tratamento com LPS. Níveis de Iba1, fosforilação de NF-kB e expressão de IL1b e TNFa retornam aos níveis de controle 5 meses após a injeção. Estas diferenças na manutenção do estado inflamatório podem ser explicadas pela resposta estrutura-específica e a diferença de densidade de células gliais entre as diferentes regiões.

2. Inflamação hipocampal leva a perda neuronal e alterações sinápticas

Define-se neuroinflamação como um conjunto de alterações no cérebro, incluindo ativação glial e secreção de mediadores inflamatórios. Tal condição é uma das principais características ambientais de desordens neurodegenerativas responsável pela geração de um ambiente neurotóxico (Ransohoff et al., 2016). A neuroinflamação, em um primeiro momento, serve como um mecanismo de defesa que protege o cérebro de danos teciduais e patógenos (Wyss-Coray et al., 2002). No entanto, a neuroinflamação crônica, com persistentes fenótipos microgliais e astrocitários inflamatórios, leva a inibição de processos regenerativos (Russo et al., 2016, Kempuraj et al., 2016) e promove a perda neuronal (Qin et al., 2007, Gasparotto et al., 2018, Zhao et al., 2019).

Costumeiramente, uma classificação dicotômica é utilizada para diferenciar os diferentes estados das células gliais: fenótipo pró-inflamatório e neurotóxico (M1 para microglia reativa, A1 para astrócitos reativos) ou um fenótipo neuroprotetor e anti-inflamatório (M2 para microglia regulatória, A2 para astrócitos regulatórios). O uso de classificação simplificadas e diretas é extremamente atrativo; no entanto, não

reflete a realidade. Astrócitos e microglia assumem diferentes fenótipos, sua classificação se encaixa mais corretamente em um espectro do que forma binária (Kown et al., 2020, Escartin et al., 2021). GFAP é um dos marcadores astrocitários mais utilizados. No entanto, níveis elevado de GFAP não representam um marcador definitivo de um fenótipo pró-inflamatório (Escartin et al., 2021). Os níveis desta proteína variam nas diversas estruturas cerebrais; por exemplo, a densidade de células GFAP positivas é maior no hipocampo (Haim et al., 2017). Iba1 é um marcador de ativação microglial empregado por diversos pesquisadores. No entanto, sua expressão é relativa a toda microglia, não só a ativada (Hopperton et al., 2018). Em ambos os casos, marcadores proliferativos deveriam ser utilizados para confirmar o recrutamento e proliferação de células gliais (Kwon et al., 2020, Escartin et al., 2021). Desta forma, mudanças nos níveis destes marcadores por si só não representa ativação glial e nem pode ser ligada a um estado neurotóxico ou neuroprotetor. Todavia, o aumento de outros parâmetros inflamatórios observados (atividade de NF-kB, aumento da expressão de IL1b e TNFa) fornecem evidências de um ambiente neurotóxico induzido pelo tratamento com LPS.

Células da microglia representam cerca de 12% da população no cérebro, com densidades variadas entre as regiões cerebrais (0,5% a 16,6%); regiões como os gânglios da base e o hipocampo possuem uma alta densidade de microglia (Block et al., 2007). Diversos estímulos são capazes de ativar a microglia desencadeando grandes alterações na morfologia e funções celulares (Nimmerjahn et al., 2005, Fetler et al., 2005). Ativação microglial serve um propósito neuroprotetor: “vigilância ambiental” (limpeza de moléculas neurotóxicas no citoplasma), sobrevivência neuronal através da liberação de fatores tróficos e anti-inflamatórios e resposta imune inata (Simard et al., 2006, Town et al., 2005, Lial et al, 2005, Streit et al.,

2002). No entanto, uma super ativação microglial se torna neurotóxica levando ao aumento da produção de radicais livres, aumento da atividade de NF-kB e do inflamassoma, e níveis elevados de citocinas pró-inflamatórias (Kwon et al., 2020, Ransohoff et al., 2016, Wyss-Coray et al., 2002)

3. Relação Inflamação-Neurodegeneração-Sono

Diferentemente de humanos, os roedores possuem sono polifásico, e ainda que seja de difícil classificação o início e término de cada ciclo do sono, as características de sono REM e NREM são bem definidas (Phillips et al., 2010, Simasko et al., 2009). O sono REM é caracterizado pela predominância de ondas Theta (5-10 Hz) no registro de LFP hipocampal, com pico em 7 Hz na fase tônica e atonia muscular (Jing et al., 2016). O sono NREM é caracterizado pela dominância de ondas Delta (1-4 Hz) no LFP hipocampal, um pico em 2 Hz e atonia muscular (Jing et al., 2016). No entanto, a inflamação é capaz de alterar tais parâmetros. Animais submetidos a cirurgia de indução de sepse (ligadura e punção cecal) e animais submetidos à endotoxemia por LPS demonstram redução no sono REM (Baracchi et al., 2011, Nachón-García et al., 2018). Soma-se a isto, que a administração das citocinas pró-inflamatórias IL1b e TNFa levam a indução do sono NREM e redução do sono REM (Krueger et al., 2008). Insultos inflamatórios também são capazes de modular a atividade cerebral fisiológica. Ratos Lister Hooded tratados com LPS demonstram uma redução na frequência média de Theta e Delta, e redução do pico de Theta no hipocampo (Mamad et al., 2017).

Os experimentos conduzidos neste estudo demonstraram uma redução no poder de Theta durante o sono REM juntamente a uma diminuição da duração dos

episódios deste tipo de sono. Não foi possível observar diferenças no pico de Delta durante o sono NREM e nem no pico de Theta durante o sono REM. No mesmo período foi possível observar uma elevação na expressão das citocinas pró-inflamatórias IL1b e TNFa, indicando uma relação temporal entre o aumento dos níveis de parâmetros inflamatórios e alterações no sono REM. As citocinas IL1b e TNFa são capazes de induzir o sono NREM e perturbar o sono REM (Besedovsky et al., 2019). Quando expostos a privação de sono, há uma elevação na produção destas citocinas para que um mecanismo compensatório leve estes animais a dormir mais, buscando a homeostase do sono; animais *knockout* para IL-1R1 e TNFR1 não são capazes de evocar este efeito rebote (Baracchi et al., 2008). Além disso, animais *knockout* para IL-1R1 não são responsivos à estimulação de Theta (Avital et al., 2003). Nossos resultados sugerem um papel para citocinas pró-inflamatórias na modulação do sono REM de animais tratados com LPS meses após a exposição.

A atividade de Theta hipocampal é de extrema relevância para mecanismos associados à memória emocional. A coerência entre a atividade de Theta hipocampal e da amígdala desencadeia expressão gênica relacionada à plasticidade, indicando um papel do sono REM na consolidação da memória emocional (Hutchison et al., 2015). A sinaptofisina, cujo os níveis foram reduzidos em decorrência do tratamento com LPS, é uma proteína associadas a vesículas pré-sinápticas, a redução dos seus níveis está associada a alterações em mecanismos relacionados à plasticidade como a perda da potenciação de longo termo (LTP) (Li et al., 2012, Janz et al., 1999). A LTP é um mecanismo importante na plasticidade e consolidação da memória. (Lynch et al., 2004). Estudos anteriores demonstraram déficits cognitivos e de memória em animais tratados com LPS (Zhao et al., 2019, Joshi et al., 2014), além de alterações na neurogênese adulta, outro

mecanismo relacionado à memória e plasticidade (Perez-Dominguez et al., 2019). Investigações sobre mecanismos de plasticidade e testes comportamentais podem revelar a que nível o tratamento com LPS pode prejudicar a consolidação da memória.

Estudos anteriores demonstraram que lesões hipocampais afetam a qualidade do sono (Spanò et al., 2020); tendo em vista a relação bidirecional entre sono e neurodegeneração, estudos também já demonstraram que a privação de sono causada por apnéia inibe a função hipocampal e a neurogênese adulta (Navarro-Sanchis et al., 2017, Mueller et al., 2008). Além disto, pacientes de RBD idiopático também apresentam atrofia hipocampal (Campabadal et al., 2019). A depressão, outro sintoma não-motor característico da DP, afeta cerca de 50% daqueles acometidos por esta desordem (Reijnders et al., 2008). A atrofia hipocampal também está diretamente relacionada com a severidade das características clínicas de desordens depressivas (Sheline et al., 2011). O sono e a depressão, duas características de extrema relevância no contexto da DP, se relacionam com a disfunção, atrofia e degeneração do hipocampo. No entanto, modelos da DP tendem a ignorar a relevância dos processos degenerativos que ocorrem em outras regiões do cérebro fora o eixo dopaminérgico por compreenderem uso de substâncias que levam a uma perda neuronal aguda através da administração intracranial em regiões específicas (Tieu et al., 2011). Por este motivo, é necessária a utilização de modelos que propriamente mimetizam as disfunções que ocorrem por todo o cérebro na DP, para que se possa responder diversas perguntas que foram levantadas desde a primeira descrição da DP.

.

Conclusão

Ratos Wistar de 50 dias tratados com LPS são acometidos por um estado neuro-inflamatórios no hipocampo 3 meses após a exposição a esta endotoxina. A neuro-inflamação foi caracterizada pelos níveis elevados de Iba1, RAGE, atividade de NF-kB e níveis elevados de expressão das citocinas IL1b e TNFa. Estas citocinas estão estritamente relacionadas com a modulação de parâmetros do sono. Elevados níveis de citocinas pró-inflamatórios tem uma relação temporal com episódios mais curtos de sono REM e diminuição do poder de Theta durante o sono REM. Estes resultados indicam que o tratamento com LPS sistêmico leva a uma disrupção do sono REM meses depois de um insulto inflamatório sistêmico através da manutenção de um estado inflamatório crônico no cérebro. Parâmetros inflamatórios e do sono retornaram a níveis de controle 5 meses após a exposição ao LPS.

A prolongada neuro-inflamação culminou em neurodegeneração e alterações sinápticas no hipocampo dos animais tratados com LPS. Foi possível observar uma redução nos níveis de NEFL, NeuN e Sinaptofisina. Tais resultados realçam a possibilidade do uso de alterações neuro-inflamatórias e do sono para indicar populações de risco para desordens neurodegenerativas e a possibilidade translacional de modelos animais.

.

Perspectivas

Nossos resultados demonstram uma clara modulação do sono REM por mediadores inflamatórios em decorrência do tratamento sistêmico com LPS. Diversos autores já demonstraram a importância do sono REM na consolidação de memórias emocionais (Kumar et al., 2020, Lipinska et al., 2019, Pesonen et al., 2019). Um dos questionamentos que estes resultados nos trazem é a que nível estas alterações no sono REM estão afetando o comportamento e a consolidação da memória destes animais. É de interesse do grupo avaliar comportamentos do tipo depressivo e ansioso em animais tratados com LPS por meio de testes como o teste de campo aberto, teste do nado forçado e teste de preferência por sacarose e o teste de *splash*. Além disso, existe o interesse em realizar tarefas como o labirinto aquático de Morris (memória espacial) e o teste de condicionamento de medo contextual e sugerido (memória emocional).

Apesar da elevação de diversos parâmetros inflamatórios que indicam uma ativação microglial e um estado neuro-inflamatório no hipocampo, um perfil inflamatório mais completo seria possível através de análises de microscopia de imunofluorescência para diversas proteínas ligadas a proliferação, recrutamento e ativação glial como GFAP, S100b, Iba1, Nestina, Ki67 e PCNA (Escartin et al., 2021, Kwon et al., 2020). Da mesma forma, análises de microscopia também poderiam fornecer resultados interessantes sobre perda neuronal e degeneração axonal através de marcadores como NeuN, NEFL e b-3-tubulina. A utilização de marcadores associados a neurônios imaturos e jovens, como a doublecortina, também permitiria avaliar possíveis disrupções na neurogênese adulta.

Trabalhos anteriores já demonstraram a influência do RAGE para a neuroinflamação e futura perda neuronal no modelo do LPS sistêmico (Gasparotto et al., 2017, Gasparotto et al., 2018). Uma possível intervenção com um inibidor farmacológico de RAGE, FPS-ZM1, poderia inibir a inflamação hipocampal levando a normalização dos parâmetros do sono e evitando uma possível neurodegeneração.

Referências

1. Burlá C, Camarano A A, Kanso S, Fernandes D, Nunes R, Panorama prospectivo das demências no Brasil: um enfoque demográfico, Cienc Saúde Coletiva 2013; 18(10): 2949-2956
2. Erkkinen MG, Kim MO, Geschwind MD. Clinical Neurology and Epidemiology of the Major Neurodegenerative Diseases. Cold Spring Harb Perspect Biol. 2018 Apr 2;10(4):a033118. doi: 10.1101/cshperspect.a033118.
3. Fjell AM, Sørensen Ø, Amlien IK, Bartrés-Faz D, Bros DM, Buchmann N, Demuth I, Drevon CA, Düzel S, Ebmeier KP, Idland AV, Kietzmann TC, Kievit R, Kühn S, Lindenberger U, Mowinckel AM, Nyberg L, Price D, Sexton CE, Solé-Padullés C, Pudas S, Sederevicius D, Suri S, Wagner G, Watne LO, Westerhausen R, Zsoldos E, Walhovd KB. Self-reported sleep relates to hippocampal atrophy across the adult lifespan: results from the Lifebrain consortium. Sleep. 2020 May 12;43(5):zsz280. doi: 10.1093/sleep/zsz280. PMID: 31738420; PMCID: PMC7215271.
4. GBD 2016 Dementia Collaborators, Global, regional, and national burden of Alzheimer's disease and other dementias, 1990–2016: a systematic analysis for the Global Burden of Disease Study 2016, Lancet Neurol 2019; 18:888-106

5. Guo Y, Cai H, Chen L, Liang D, Yang R, Dang R, Jiang P. Quantitative profiling of neurotransmitter abnormalities in the hippocampus of rats treated with lipopolysaccharide: Focusing on kynurenine pathway and implications for depression. J Neuroimmunol. 2016 Jun 15;295-296:41-6. doi: 10.1016/j.jneuroim.2016.04.006. Epub 2016 Apr 14. PMID: 27235347.
6. Gustot A, Gallea JI, Sarroukh R, Celej MS, Ruysschaert JM, Raussens V. Amyloid fibrils are the molecular trigger of inflammation in Parkinson's disease. Biochem J. 2015 Nov 1;471(3):323-33. doi: 10.1042/BJ20150617. Epub 2015 Aug 13. PMID: 26272943.
7. Lee HJ, Suk JE, Patrick C, Bae EJ, Cho JH, Rho S, Hwang D, Masliah E, Lee SJ. Direct transfer of alpha-synuclein from neuron to astroglia causes inflammatory responses in synucleinopathies. J Biol Chem. 2010 Mar 19;285(12):9262-72. doi: 10.1074/jbc.M109.081125. Epub 2010 Jan 13. PMID: 20071342; PMCID: PMC2838344.
8. Lema Tomé CM, Tyson T, Rey NL, Grathwohl S, Britschgi M, Brundin P. Inflammation and α-synuclein's prion-like behavior in Parkinson's disease--is there a link? Mol Neurobiol. 2013 Apr;47(2):561-74. doi: 10.1007/s12035-012-8267-8. Epub 2012 Apr 29. PMID: 22544647; PMCID: PMC3589652.
9. Li Q, Haney MS. The role of glia in protein aggregation. Neurobiol Dis. 2020 Sep;143:105015. doi: 10.1016/j.nbd.2020.105015. Epub 2020 Jul 12. PMID: 32663608.
10. Lipton SA, Gu Z, Nakamura T. Inflammatory mediators leading to protein misfolding and uncompetitive/fast off-rate drug therapy for neurodegenerative

disorders. Int Rev Neurobiol. 2007;82:1-27. doi: 10.1016/S0074-7742(07)82001-0. PMID: 17678953.

11. Lotharius J, Brundin P. Pathogenesis of Parkinson's disease: dopamine, vesicles and alpha-synuclein. Nat Rev Neurosci. 2002 Dec;3(12):932-42. doi: 10.1038/nrn983. PMID: 12461550.
12. Loyola Filho A I, Matos D L, Giatti L, Afradique M E, Peixoto S V, Lima-Costa M F, Causas de internações hospitalares entre idosos brasileiros no âmbito do Sistema Único de Saúde, Epidemiol Serv Saúde 2004; 13(4):229-238
13. Phillips AJ, Robinson PA, Kedziora DJ, Abeysuriya RG. Mammalian sleep dynamics: how diverse features arise from a common physiological framework. PLoS Comput Biol. 2010 Jun 24;6(6):e1000826. doi: 10.1371/journal.pcbi.1000826. PMID: 20585613; PMCID: PMC2891699.
14. Prince, M., et al., World Alzheimer Report 2015: The Global Impact of Dementia. An analysis of prevalence, incidence, cost and trends. 2015, Alzheimer’s Disease International: London.
15. Shattuck EC, Muehlenbein MP. Human sickness behavior: Ultimate and proximate explanations. Am J Phys Anthropol. 2015 May;157(1):1-18. doi: 10.1002/ajpa.22698. Epub 2015 Jan 13. PMID: 25639499.
16. Simasko SM, Mukherjee S. Novel analysis of sleep patterns in rats separates periods of vigilance cycling from long-duration wake events. Behav Brain Res. 2009 Jan 23;196(2):228-36. doi: 10.1016/j.bbr.2008.09.003. Epub 2008 Sep 16. PMID: 18835301; PMCID: PMC2617706.
17. Zahra W, Rai SN, Birla H, Singh SS, Dilnashin H, Rathore A S, The Global Economic Impact of Neurodegenerative Diseases: Opportunities and

Challenges In: Keswani C (eds) Bioeconomy for Sustainable Development Springer, 2020

18. Zhang W, Wang T, Pei Z, Miller DS, Wu X, Block ML, Wilson B, Zhang W, Zhou Y, Hong JS, Zhang J. Aggregated alpha-synuclein activates microglia: a process leading to disease progression in Parkinson's disease. FASEB J. 2005 Apr;19(6):533-42. doi: 10.1096/fj.04-2751com. PMID: 15791003.

Anexo I

Artigo submetido ao periódico

"Neurochemistry International"

Hypoxia inducible factor-1*α* (HIF-1*α*) inhibition impairs retinoic acid induced differentiation in SH-SY5Y neuroblastoma cells, leading to reduced neurite length and diminished gene expression related to cell differentiation.

Pedro Ozorio Brum [a⁺], Guilherme Danielski Viola [c], Carolina Saibro-Girardi [a], Camila Tiefensee-Ribeiro [a], Matheus Ozorio Brum, Juciano Gasparotto[a], Rachel Krolow [b], José Cláudio Fonseca Moreira [a], Daniel Pens Gelain [a].

[a] Centro de Estudos em Estresse Oxidativo, Departamento de Bioquímica, Instituto de Ciências Básicas da Saúde, Universidade Federal do Rio Grande do Sul – Porto Alegre, RS – Brazil;

[b] Laboratório de Programação Neurobiológica do Comportamento Alimentar, Departamento de Bioquímica, Instituto de Ciências Básicas da Saúde, Universidade Federal do Rio Grande do Sul – Porto Alegre, RS – Brazil;

[c] Laboratório de Medicina Genômica, Centro de Pesquisa Experimental, Hospital de Clínicas de Porto Alegre – Porto Alegre, RS – Brazil.

[⁺]Corresponding author

*Mailing address: Rua Ramiro Barcelos, 2600 – anexo, CEP 90035-003, Porto Alegre, RS, Brazil. Phone: +55 51 3308-5577, Fax: +55 51 3308-5535.

e-mail: pedrobrum1@gmail.com

Abstract: Neuroblastoma is the most common extracranial solid tumor in childhood, originated from cells of the neural crest during the development of the Sympathetic Nervous System. Retinoids are vitamin-A derived differentiating agents utilized to avoid disease resurgence in high-risk neuroblastoma treatment. Several studies indicate that hypoxia - a common feature of the tumoral environment - is a key player

in cell differentiation and proliferation. Hypoxia leads to the accumulation of the hypoxia inducible factor-1***α*** (HIF-1***α***). This work aims to investigate the effects of the selective inhibition of HIF-1***α*** on the differentiation induced by retinoic acid in human neuroblastoma cells from the SH-SY5Y lineage, with the purpose of clarifying its role in cell differentiation. Our results indicated that HIF-1***α*** inhibition impairs RA-induced differentiation through reduction of neuron-like phenotype and diminished immunocontent and expression of differentiation markers.

Keywords: Hypoxia, differentiation, neuroblastoma, cancer, HIF-1, SH-SY5Y

1. Introduction

Neuroblastoma (NB) is a heterogeneous pediatric solid tumor with various forms, which range from extremely aggressive metastatic cancer - with cure rates as low as <50% - to low-risk disease - with chances of a good prognosis greater than 90% (1). NB arises from the neural crest (NC) during the formation of the sympathetic

nervous system (SNS) (2). Despite its low incidence, NB is responsible for 10% of child cancer deaths (3) and is the most common extracranial solid tumor in childhood (1). High-risk NB treatment includes high-dose myeloablative chemotherapy followed by stem cell rescue, radiation, surgery, and retinoid treatment to avoid cancer resurgence (23, 24).

Hypoxia and hypoxia inducible factors' (HIFs) elevated expression is a common feature of the tumoral environment (25, 26). The hypoxia inducible factor-1 (HIF-1) is a cell-sensor to oxygen concentrations, targeting gene expression related to cell fate. HIF-1 is a heterodimer composed of its ***α*** and β subunits. ***α*** subunit's stability, cellular location, and expression are directly related to oxygen levels. In contrast, the β subunit, also known as aryl hydrocarbon receptor nuclear translocator (ARNT), is constitutively expressed and is not oxygen-sensible (6). Once the β subunit dimerizes with HIF-1***α***, HIF-1 binds to hypoxia responsive elements (HRE) and promotes gene expression related to angiogenesis, erythropoiesis, metabolism, and cell proliferation and survival. In normoxic conditions, the ***α*** subunit is degraded in a process of von-Hippel-Lindau protein (pVHL) mediated ubiquitin-proteasome pathway, which is inhibited by hypoxia (27). The interaction between HIF-1***α*** and pVHL is triggered by the post-translational hydroxylation of HIF-1***α*** by prolyl hydroxylase (PHD) (12). HIF-PHD hydroxylases HIF-1***α*** in oxygen-dependent degradation domains (ODD). These post-translational modifications to HIF-1***α*** allow for pVHL binding - an E3 ubiquitin ligase - leading to ubiquitination and further proteasomal degradation (28).

Besides its fine oxygen-dependent regulation, few other factors seem to stabilize HIF-1***α***. Proinflammatory stimuli may lead to a PI3K/Akt/mTOR-mediated increase in *HIF1A* expression (7). Hypoxia-mimetic agents such as deferoxamine

(DFO) (8) and $CoCl_2$ (10) are capable of stabilizing HIF-1***α*** through the inhibition of PHD. HIF-1***α*** activity is sensible to changes within cell energetic metabolism. Citric acid cycle dysfunction and accumulation of its intermediaries lead to inhibition of HIF-1***α*** hydroxylases and therefore results in HIF-1***α*** stabilization bypassing the oxygen-dependent regulation (13, 32, 33). Studies have shown that retinoic acid administration in different cell types leads to HIF-1***α*** accumulation (10, 11) and that RA signaling might be dependent on HIF-1***α*** (5, 10, 11). RA treatment in SH-SY5Y leads to changes in cell energetic metabolism, in turn leading to increased oxidative stress (30, 34, 36). Elevated levels of oxygen-reactive species activate mitochondrial HIF-1***α*** (35), which may explain the rise in HIF-1***α*** levels after retinoic acid treatment.

Neuroblastoma cells can be induced to differentiate in a neuron-like phenotype. SH-SY5Y neuroblastoma cells express proliferative markers such as the immature neuronal marker nesting and the proliferating cell nuclear antigen (PCNA). When treated with retinoic acid (RA), these cells exhibit a neuron-like phenotype with extensive projections, cell-cycle arrest, and the expression of neuronal markers such as enolase 2 (*ENO2*), synaptophysin (*SYP*) and the microtubule-associated protein tau (*MAPT*/*TAU*) (15). SH-SY5Y are known for a catecholaminergic phenotype upon differentiation, expressing dopaminergic markers such as tyrosine hydroxylase (*TH*), dopamine transporter (*DAT*) and exhibit moderate levels of dopamine-β-hydroxylase (*DßH*) activity (16, 17). RA-treated SH-SY5Y cultures lack the expression of glial markers such as the glial fibrillary protein (GFAP) (15). While SH-SY5Y neuroblastoma cells exposed to the hypoxia mimetic agent deferoxamine (DFO) express a neuron-like tyrosine hydroxylase (TH) expressing phenotype (8), NB1691 neuroblastoma cells exposed to intermittent hypoxia expressed increased NC markers and decreased SNS markers, even though there was an increase in TH.

Under RA treatment and hypoxia exposure NB1691 cells demonstrated diminished responsiveness to differentiation induced by RA (14). In the same study, the authors demonstrated that HIF-1***α*** inhibition under intermittent hypoxia conditions leads to an increase in a neuron-like phenotype in NB1691 cells. These findings contrast to the work of Cimmino et al (5), who have demonstrated a diminished neuron-like phenotype in HIF-1***α*** silenced neuroblastoma cells - SH-SY5Y, SKNBE2c, SKANS - exposed to RA under normoxic conditions.

The purpose of our study was to determine HIF-1***α***'s role in retinoic acid induced differentiation in SH-SY5Y cell cultures under normoxic conditions. For such, we *silenced* HIF-1***α*** expression through small interference RNA (siRNA) and exposed the cell cultures to a 7 days RA-induced differentiation protocol. Our results indicate that HIF-1***α*** inhibition impairs RA-induced differentiation through reduction of neuron-like phenotype and diminished immunocontent and expression of differentiation markers.

2. Methods

2.1 Cell Culture and Differentiation

Human neuroblastoma SH-SY5Y were obtained from the ECACC (European Collection of Cell Culture) and were grown in DMEM/F12 (Sigma-Aldrich - D8900) containing 10% fetal bovine serum (FBS) at 37°C in 5% CO2 and 95% air in a humidified atmosphere. Differentiation cells were plated at 10^3 cells/cm^2 confluency and treated with retinoic acid at 10μM concentration in DMEM/F12 1% FBS for 7 days with retinoic acid pulses at days 1, 4 and 7.

2.2 siRNA knockdown

HIF-1***α*** small interference RNA Silencer ® Select at 5nM (Ambion - 4392420, ID: n336610) and siRNA scramble (Ambion - AM4635) as control at 30 nM were transfected using the reverse transfection protocol with siPORT™ NeoFX™ Transfection Agent (Ambion®, Applied Biosystems Inc.) and Opti-MEM following manufacturer's instructions. Cells were transfected in DMEM/F12 medium with 10% FBS without antibiotics. Knockdown efficiency was evaluated through RT-qPCR and Western Blot. Cells were transfected 24 hours prior to retinoic acid treatment (day 0).

2. 3 Treatment Timeline

Experiments were performed on a 9-day timespan beginning on day 0 through day 9 (Fig. 1 A). On day 0, cells were trypsinized and transfected with siRNA (siRNA scramble or siRNA HIF1***α***) at a confluence of 10^3 cells/cm^2. After 24 hours (day 1), either (i) transfection cells were either collected for RT-qPCR or western blot in order to validate transfection efficiency or (ii) RA treatment was initiated. Retinoic acid pulses were administered within 72 hours intervals (days 1, 4 and 7). Cells were either collected for RT-qPCR or fixed for immunofluorescence microscopy 24 hours after the last pulse (day 8).

2.4 Western Blot

For western blot analysis cells were lysed in 4X Laemmli buffer (250 mM Tris, 8% SDS, 40% glycerol and 0.002% bromophenol blue, pH 6.7), and then vigorously vortexed and boiled for ten minutes at 100°C. Samples were loaded and separated in 10% polyacrylamide gel and then electro-blotted to nitrocellulose membranes. Protein loading and electroblotting efficiency were verified through Ponceau S staining. Membranes were washed in Tris-buffered saline Tween-20 (Tris 100 mM, pH 7.5, 0.9% NaCl and 0.1% Tween-20) and blocked in TBS-T with 5% BSA. Membranes were washed three times post-blocked and then incubated overnight at

4°C with primary antibodies (all primary antibodies were used at 1:1000 dilution) for HIF-1***α*** (Cell Signaling - 141795) and **β**-actin (Sigma-Aldrich - A1978). Subsequently, membranes were incubated with the corresponding species-specific secondary antibody (all secondary antibodies were used at 1:2000 dilution) coupled to peroxidase (Sigma-Aldrich - AP132P; AP124P) following chemiluminescence detection utilizing the Westar Nova 2.0 kit (Cyanagen - XLS071,0250) and the GE® ImageQuant LAS 4000 CCD camera to obtain images.

2.5 Immunofluorescence

Cells were fixed in 4% paraformaldehyde for 10 minutes at room temperature followed by a 10 minute permeabilization utilizing ice-cold 0.1% Triton-PBS. In order to block nonspecific binding, cells were incubated with 1% albumin, 22.52 mg/mL glycine in T-PBS (PBS + Tween 20 0,1%) for 1 hour at room temperature. Cells were then incubated overnight with primary antibodies for glial fibrillary protein (GFAP) (Sigma-Aldrich - G6171) and Neurofilament-L (NEFL) (Cell Signaling - 2837) (all primary antibodies were used at 1:500 dilution), followed by a 1-hour incubation with its specie-specific corresponding secondary antibody coupled with Alexa Fluor® staining (488 nm or 555 nm) from Cell Signaling Technology® at room temperature (all secondary antibodies were used at 1:500 dilution). Cells were then incubated for 5 minutes with DAPI for nucleic acid staining (1:1000; D9542 - Sigma-Aldrich®). Following each step, cells were washed 3 times for 5 min in ice-cold PBS. Images were obtained through a Microscopy EVOS® FL Auto Imaging System

(AMAFD1000 - Thermo Fisher Scientific®). Immunocontent was measured as fluorescence intensity and was quantified utilizing the software ImageJ measuring the pixels of images with 100 µm of magnification. Total number of neurites per cell and

the average size of neurites were obtained with NeuronJ, an ImageJ plugin with 400 µm magnification.

2.6 Real Time-qPCR

Cells were collected utilizing the TRIzol reagent (Thermo Fisher Scientific) and RNA extractions were conducted following the manufacturer's instructions. cDNA synthesis was performed using the High Capacity cDNA Reverse Transcription kit from Applied Biosystems. Real time polymerase chain reaction was carried employing SYBR™ Green PCR Master Mix kit, 100 ng of cDNA and 100µM of each primer: *ENO2*, *SYP*, *TAU*, *HIF1A* and the housekeeping genes *GNB2L* and B2M (Table 1). Results were normalized in relation to the housekeeping genes (ΔCt) and for each case, the most stable housekeeping gene was applied. Results were expressed using the $2^{-\Delta\Delta CT}$ method.

Gene Target	Forward	Reverse
ENO2	*CTGACAAAGTCCTGGTAGAGTG*	*GATCGTTATTGGCATGGATGTTG*
SYP	*AGACAGGGAACACATGCAAG*	*TCTCCTTAAACACGAACCACAG*
TAU	*GACAGAGTCCAGTCGAAGATTG*	*AGGAGACATTGCTGAGATGC*
HIF1A	*TGATGCTTTAACTTTGCTGGC*	*TTTCAGCGGTGGGTAATGG*
GNB2L	*GAGTGTGGCCTTCTCCTCTG*	*GCTTGCAGTTAGCCAGGTTC*
B2M	*TGCTGTCTCCATGTTTGAT*	*TCTCCGCTCCCCACCTCTA*

Table 1: Sequences of the primers employed in RT-qPCR experiments.

2.7 Cohort selection and gene expression analysis

The TARGET RNA-seq dataset and clinical data from Neuroblastoma patients were downloaded from the UCSC Xena browser (https://xenabrowser.net/). The gene expression values were added 1 and then log2-transformed before analysis. The most relevant genes for this study were selected according to their respective

Ensembl number. Only samples clinically classified as stage IV were selected for future analysis. HIF1A median gene expression sets the baseline for classification of the cohort between HIF1A high (expression above median) and low (below median) expression.

2.8 Statistical Analysis

Statistical analysis was performed with the GraphPad Prism software version 7.0 (GraphPad Software Inc., San Diego, USA). Data were evaluated by one-way ANOVA followed by Tukey's Multiple Comparison *post-hoc* test or unpaired Student's t-test when suitable. Differences were considered significant when $p<0.05$.

3. Results

*3.1 siRNA transfection effectively inhibits HIF1**α** expression and diminishes its immunocontent*

Cells were maintained in DMEM/F12 10% FBS and, on day 0, cells were trypsinized for reverse transfection. Cells were seeded at a confluence of $10^3/cm^2$. After 24 hours from transfection (day 1), cells were collected for western blot or RT-qPCR to assess transfection efficiency. mRNA levels (Fig. 1E) and HIF-1**α** immunocontent (Fig. 1F) decreased when cells were transfected with 5 nM HIF-1**α** siRNA select (sHIF) in comparison to 30 nM scrambled siRNA transfected cells (sSCR) without any morphological alterations (Fig. 1B-D) that could indicate changes in cell viability. The incubation time used for all experiments was 24 hours since it showed greater effectiveness of inhibition when compared to other incubation times (data not shown).

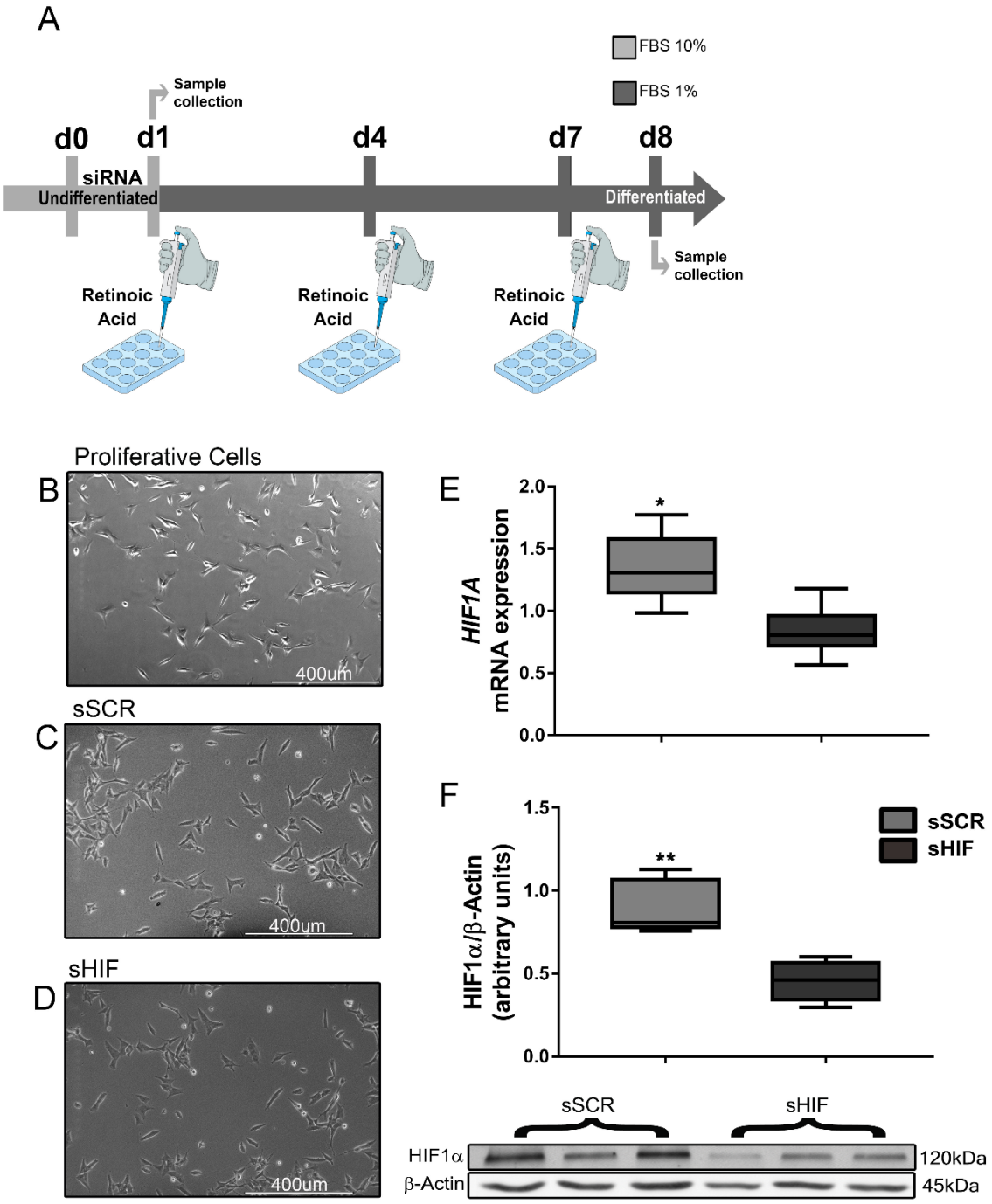

Figure 1. Cell silencing and differentiation protocol (A): Protocols were performed on a 9-day time span, from day 0 to day 7. On day 0 cells were trypsinized and seeded for reverse transfection. On day 1, either cells were collected for RT-qPCR and western blot or retinoic acid (RA) treatment was initiated on the concentration of 10 μM. On days 4 and 7, cells received RA pulses. On day 8, cells were either fixed for

immunofluorescence microscopy or collected for RT-qPCR. HIF-1***α*** siRNA transfection leads to a decrease in protein and mRNA levels without morphological alterations that could indicate changes in cell viability. (B) Phase microscopy showing cell morphology in growth conditions prior to plating and siRNA transfection. Phase microscopy showing cell morphology after siRNA transfection of both HIF-1***α*** siRNA (sHIF) (C) and scramble siRNA (sSCR) (D). In (E) HIF-1***α*** mRNA levels and (F) HIF-1***α*** protein levels after transfection. (unpaired Student's t test *p<0.01, **p<0.005).

*3.2 HIF-1**α** silencing impairs cell differentiation leading to changes in cell morphology*

Transfected cells were treated with 10μM retinoic acid for 7 days. RA pulses were administered on days 1, 4 and 7 (Fig. 1A). Undifferentiated (undiff.) cells demonstrated a triangle shaped morphology (Fig. 2A) with low average neurite length (Fig. 2E) and low total neurites/cell (Fig. 2D). sSCR cells treated with retinoic acid (sSCR + RA) demonstrated extensive neurites (Fig. 2B) with a greater neurite length average and total neurite/cell (Fig. 2D-E). HIF-1***α*** *silencing* (sHIF + RA) was capable of reducing the neuron-like phenotype induced by retinoic acid (Fig. 2C), demonstrating significantly shorter neurites (Fig. 2D) but was not capable of diminishing the total amount count per cell (Fig. 2E). These results suggest that HIF1-1***α*** *silencing* attenuates neurite elongation rather than neurite outgrowth.

3.3 *Downregulation of TAU, ENO2 and SYP in response to HIF-1**α** inhibition*

In order to assess whether HIF-1***α*** inhibition was capable of altering the expression of differentiation markers related to the retinoic acid treatment, we performed RT-qPCR for *TAU, ENO2* and *SYP.* As we can see in Fig. 2F-H, the expression of differentiation markers was reduced in sHIF + RA cells when compared to sSCR + RA cells (*TAU*:

p=0.0148 ; *ENO2*: p=0.0390 ; *SYP*: p=0.0295). However, this difference wasn't as marked as the difference between the undifferentiated proliferative cells (undiff.) and sSCR + RA cells (*TAU*: p=0.0001 ; *ENO2*: p=0.0096 ; *SYP*: p=0.0049). These results indicate that HIF-1***α*** has a role in promoting gene expression related to cell differentiation.

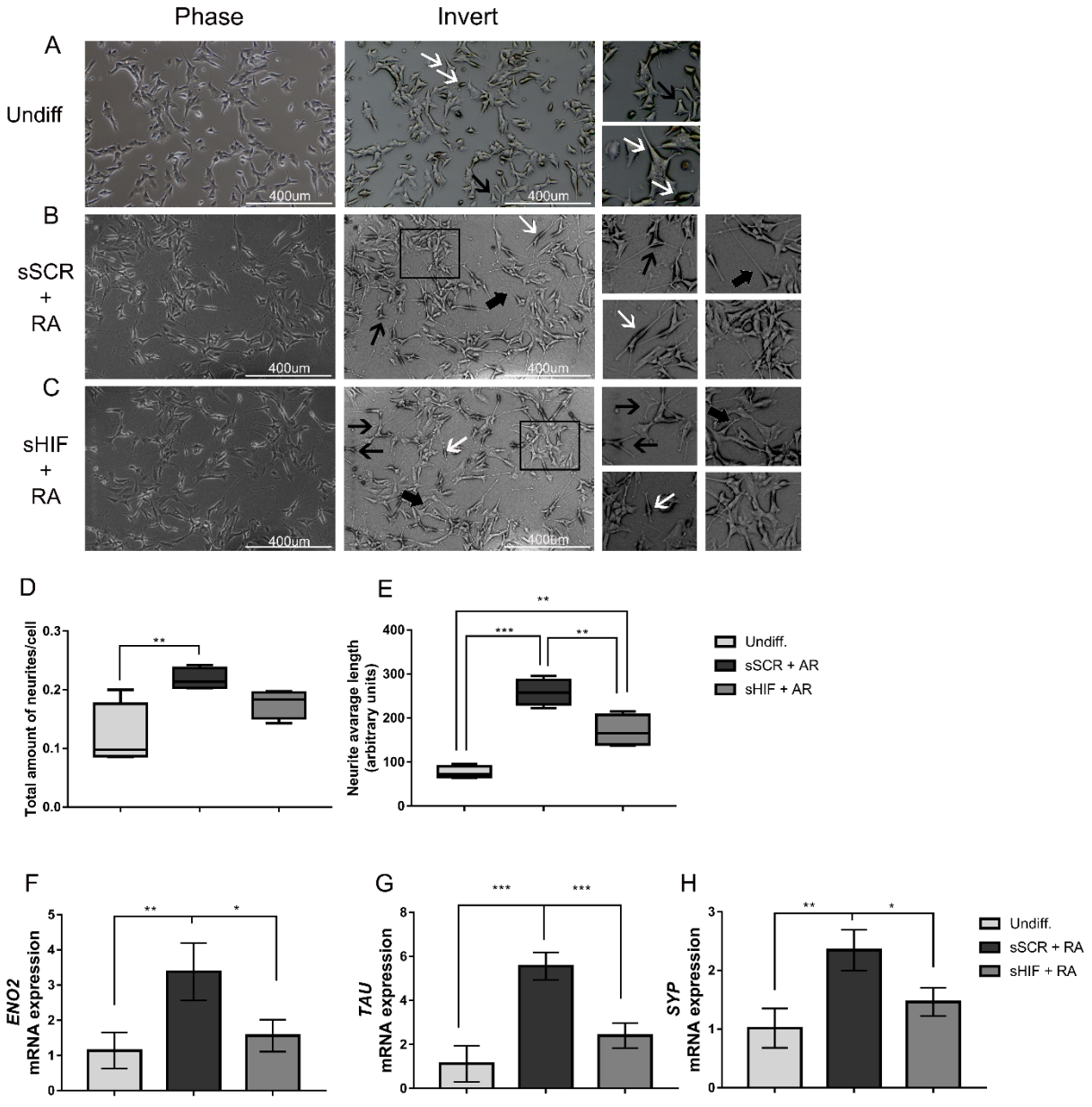

Figure 2: HIF-1***α*** inhibition affects cell differentiation. (A) Phase microscopy of undifferentiated cells demonstrating a triangular shaped phenotype. (B) sSCR + RA demonstrate extensive projections. (C) sHIF + RA demonstrate shorter projections. Total neurite/cell and neurite average length were quantified utilizing the software NeuronJ (D-E) (n=5). Cells were collected for RNA extraction and further cDNA synthesis in order to analyze neuronal markers expression through RT-qPCR (n=4). RA treatment leads to an increase in levels of F) *ENO2*, G) *SYP*, H) *TAU* in sSCR + RA when compared to undifferentiated cells and sHIF + RA cells. HIF-1***α*** *silencing* was able to reduce differentiation related gene expression. (one-way ANOVA followed by Tukey's Multiple Comparison *post-hoc* test *$p<0.05$, ***$p<0.001$).

*3.4 Inhibition of HIF-1**α** leads to diminished immunocontent of NEFL without changes in GFAP levels*

Cells were prepared for immunofluorescence staining in order to analyze the immunocontent of NEFL as a differentiation marker and GFAP as proliferative marker. As we can observe in fig. 3A-C, there were morphological changes between undiff., sSCR + RA and sHIF + RA cells. The undiff. group showed a high proliferative phenotype with a strong GFAP signal, no projections, and larger cell body area (fig. 3A). sSCR + RA cells demonstrated a highly differentiated phenotype with extensive projections and strong reactivity to NEFL antibody (fig. 3B). sHIF + RA showed reduced NEFL immunocontent and shorter projections (3C). sSCR + RA cells demonstrated a greater NEFL immunocontent when compared to both undiff. and sHIF + RA (Fig. 3D). GFAP signal showed no significant difference between all groups (fig. 3E). These results indicate that HIF-1***α*** is essential for the development of morphological features and immunocontent of differentiation markers of a neuron-like phenotype.

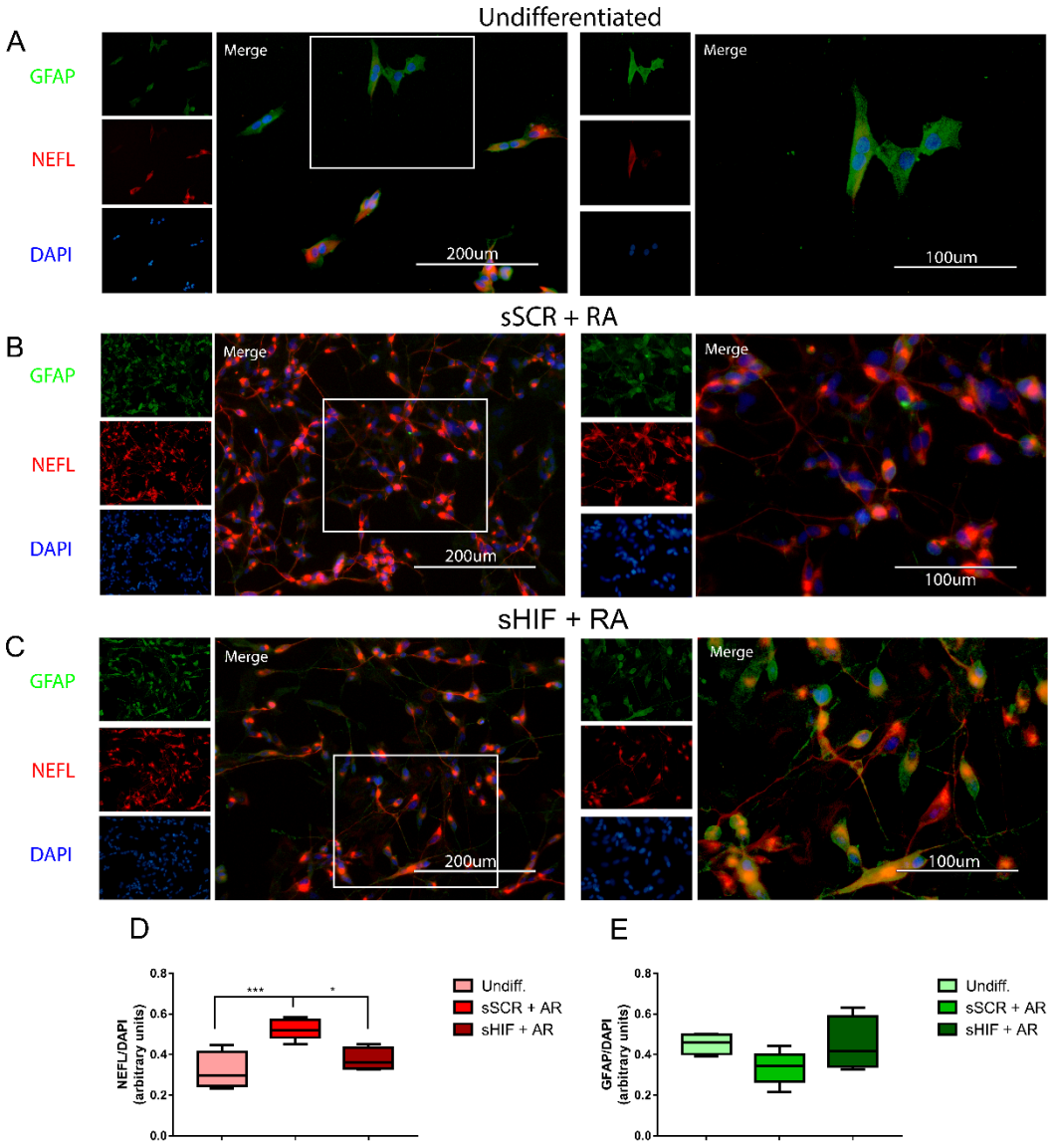

Figure 3: HIF-1***α*** inhibition led to diminished levels of NEFL and a lower average neurite length. Cells were stained for immunofluorescence with anti-NEFL antibody (red) (n=5) as a neuronal marker and anti-GFAP antibody (green) (n=5) as a proliferative marker. (A) shows the undifferentiated (undiff.) cell morphology, (B) shows sSCR + RA cells, (C) correspond to sHIF + RA cells. (D) and (E) show the fluorescence intensity of GFAP and NEFL respectively. sSCR + RA cells

demonstrated greater levels of NEFL immunocontent in comparison to Undifferentiated and sHIF + RA cells (one-way ANOVA followed by Tukey's Multiple Comparison *post-hoc* test *p<0.05, ***p<0.005).

3.5 NEFL and SYP expression is related to HIF1A expression in neuroblastoma patients

Hypoxia and the overexpression of hypoxia inducible factors is a common feature of aggressive tumors. In order to analyze the relation between *HIF1A* expression and differentiation related genes in high-risk neuroblastoma patients, we looked into gene expression data from the TARGET database. First, we classified patients into High Expression HIF1A and Low Expression HIF1A, and then assessed whether HIF1A expression is related to the worst disease outcome (Fig. 4 A-C).

We further analyzed the expression of differentiation related genes (*SYP*, *NEFL*, *ENO2*, *MAPT*) in high-risk neuroblastoma patients. The elevated expression of *HIF1A* was related to an increased mean expression of both *SYP* and *NEFL* (Fig. 4 D-E), whereas there was no change in *ENO2* and *MAPT* mean expression (Fig. F-G). These findings reinforce the results found in this study, indicating a relationship between HIF-1***α*** and differentiation markers.

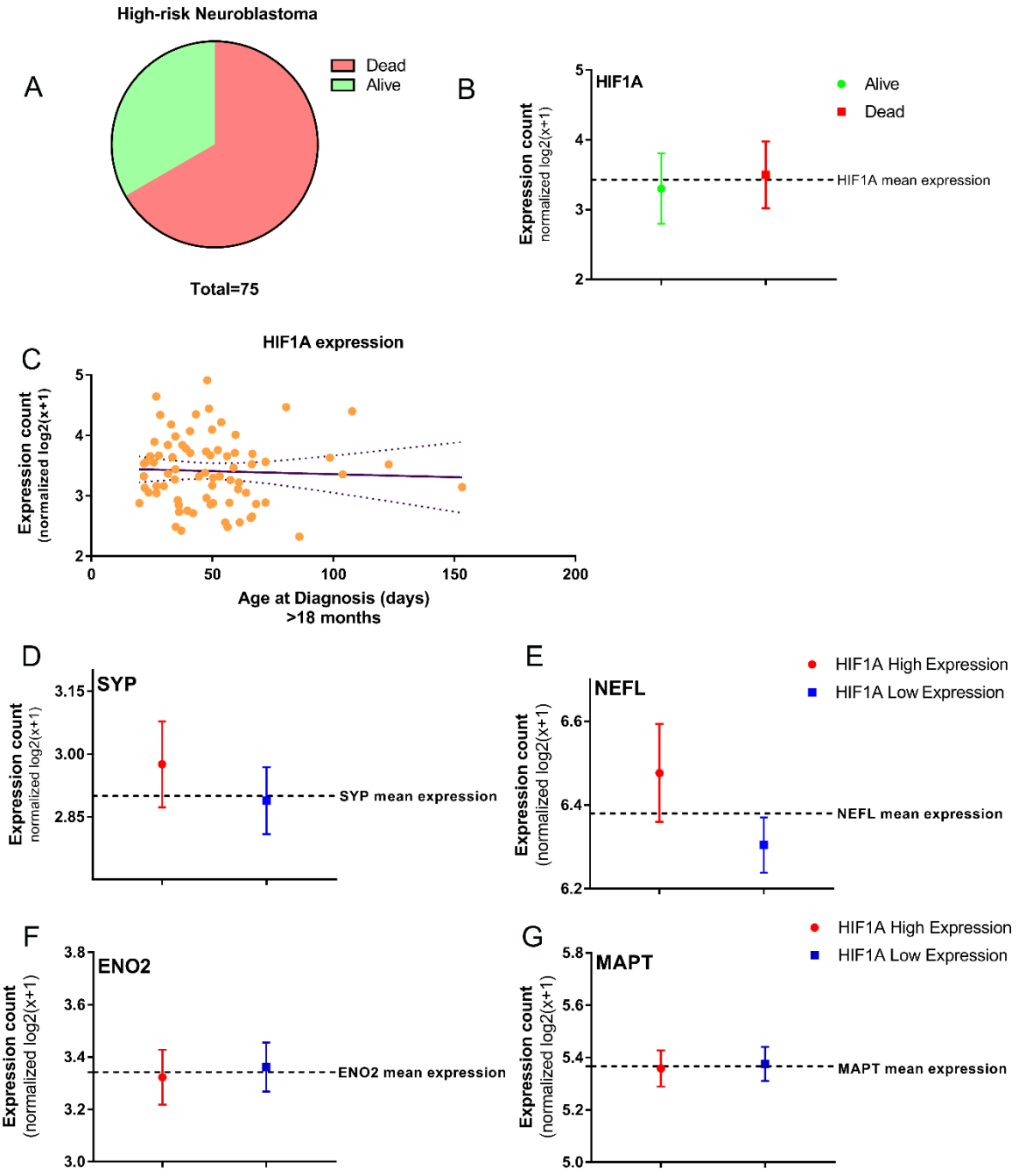

Figure 4: *HIF1A* expression was analyzed in a cohort of 75 High-Risk Neuroblastoma patients (A) in order to assess its relation to disease outcome (B) and age at diagnosis (C). *HIF1A* median expression sets the baseline for cohort classification between *HIF1A* Low Expression and *HIF1A* High Expression. We evaluated the normalized gene expression of differentiation markers *NEFL* (A), *SYP* (B), *ENO2* (C) and *MAPT* (D) in *HIF1A* High expression and *HIF1A* Low expression

patients. *NEFL* and *SYP* mean expression were elevated in *HIF1A* High-expression patients.

4. Discussion

HIF-1***α*** role in neuroblastoma cells differentiation treatment is ambiguous. Whereas in hypoxic conditions HIF-1***α*** may be responsible for RA resistance (14), it might be required for differentiation towards a neuron-like phenotype under normoxic conditions, as seen in previous findings by Cimmino and collaborators (5). In this study, we evaluated the role of HIF-1***α*** in RA-induced differentiation in neuroblastoma cells of the lineage SH-SY5Y under normoxic conditions. Our results demonstrate that HIF-1***α*** inhibition could impair the differentiation properties of RA leading to a reduced expression of differentiation markers and altered morphological features.

By RT-qPCR we demonstrated that differentiation markers such as *SYP*, *TAU* and *ENO2* were downregulated in sHIF + RA cells, even though differentiation marker presence was still higher than in undifferentiated cells. Interestingly, *SYP* and *TAU* mean expression were elevated in HIF1A Low Expression neuroblastoma patients. Our results complement the findings of Cimmino *et al* (3), who have shown that the inhibition of HIF-1***α*** leads to a reduced expression of differentiation markers *TUJ-1* and *NEFL* in retinoic acid-treated SH-SY5Y cells with lower neurite outgrowth and neurite average length. Even though we weren't able to see a significant difference in total neurite/cell between sSCR + RA and sHIF + RA cells, it is possible to observe an upward tendency in the number of neurites/cell in the sSCR + RA group. Previous studies have linked hypoxia and neuronal differentiation (19, 20). HIF-1***α*** and PHD regulate the Rho-associated protein kinase (ROCK), as inhibition of

ROCK is linked to neurite outgrowth and elongation (21, 22). HIF-1***α*** activation through $CoCl_2$ administration in mesenchymal stem cells lead to inhibition of ROCK concomitant with morphological changes and increased neuronal markers (21). This relationship between HIF-1***α*** and Rho/ROCK might explain the diminished neurite length on HIF-1***α*** *silenced* cells.

By immunofluorescence microscopy we were able to show that the inhibition of HIF-1***α*** was able to partially impair the differentiation induced by retinoic acid, showing morphological alterations such as a reduced average length of neurites combined with a lower NEFL signal. We could not observe a significant difference in GFAP levels in sSCR + RA cells. Cimmino et al (3) proposed that HIF-1***α*** inhibition leads to an enhanced glial transdifferentiation in SH-SY5Y due to an enhanced GFAP immunoconent in a 25-day treatment. In a shorter treatment of 7 days we did not observe the same alterations in GFAP levels.

Retinoic acid role in cell proliferation and differentiation is linked to HIF-1***α***, with different responses in different cell types and conditions. Zhang *et al* (10) have demonstrated an increase in HIF-1***α*** protein in response to retinoic acid treatment in myeloid leukemic cells. HIF-1***α*** conditional induction significantly increased cell differentiation, whereas HIF-1***α*** inhibition with short hairpin RNA significantly decreased cell differentiation. In neural stem and progenitor cells of the adult hippocampus, retinoic acid has a role in maintaining cell proliferation through regulation of S-phase reentry (11). Retinoic acid is known for its differentiating effect on neuroblastoma cells (15, 16, 17, 18). Oxygen levels may influence retinoic acid-HIF-1***α*** relation in neuroblastoma cells differentiation. Besides retinoic acid induction of HIF-1***α***, the response to the inhibition of this factor varies. Bhaskara et al (14) have shown that in an intermittent hypoxia (IH) model retinoic acid reduces the

differentiation towards a neuron-like phenotype. Futhermore, the authors demonstrated that HIF-1***α*** inhibition in IH is capable of inducing neuron-like characteristics. In the current study we have demonstrated that HIF-1***α*** inhibition in normoxic conditions attenuates the retinoic acid differentiation in neuroblastoma cells accompanied by reducing neurite average length, NEFL immunocontent, and *SYP*, *TAU*, *ENO2* expression. The findings of Cimmino et al (5) corroborate our results, showing a reduction in cell differentiation towards a neuron-like phenotype. However, Cimmino et al (5) assert that morphological alterations such as the appearance of flat cells forming ganglion-like structures concurrent with an enhanced GFAP signal indicate that HIF-1***α*** inhibition followed by RA treatment leads to enhanced glial transdifferentiation.

Markers such as *NEFL*, *TAU*, *SYP*, *ENO2* are commonly used by several authors to determine neuroblastoma cell differentiation *in vitro* (5, 29, 30). While these markers *in vitro* may suggest success in retinoic acid treatment, they may have different relevance for neuroblastoma patients. Immunohistochemistry of neuroblastoma tumors demonstrates that (i) synaptophysin is constitutively expressed by neuroblastoma tumoral cells, (ii) *NEFL* is a common but with inefficient mutation in neuroblastoma tumors and (iii) neuron-specific enolase (*ENO2*) is a non-favorable marker. Analyzing a cohort of 75 high-risk neuroblastoma, we observed that an elevation in the mean expression of *HIF1A* results in a higher mean expression of both *NEFL* and *SYP* (Fig. 4 D-E). Further studies are needed to explain HIF-1***α***'s role in retinoid therapies and whether these alterations in *NEFL* and *SYP* levels in HIF1A High Expression patients are beneficial.

5. Conclusion

In conclusion, we show that, HIF-1***α*** inhibition partially inhibits retinoic acid-induced differentiation in SH-SY5Y cells. HIF-1***α*** silencing was able to significantly change the morphology of retinoic acid treated neuroblastoma cells as well as to reduce the expression of differentiation markers. These findings suggest that HIF-1***α*** is involved in retinoic acid-induced differentiation regulation and may provide grounds for further studies about this transcription factor role in cell differentiation. The tumoral microenvironment presents fluctuations in oxygen levels within the tumor; hence, HIF-1***α*** has a vital role as oxygen sensor in cancer cells. Understanding how HIF-1***α*** influences cell proliferation and differentiation may provide basis for better comprehension of its influence in retinoid therapies for the treatment of neuroblastoma.

6. Funding Acknowledgement

This project was funded by Conselho Nacional de Desenvolvimento Científico e Tecnológico (CNPq), Fundação de Amparo à Pesquisa do Estado do Rio Grande do Sul (FAPERGS), Coordenação de Aperfeiçoamento Pessoal de Nível Superior (CAPES) and Pró-Reitoria de Pesquisa - Universidade Federal do Rio Grande do Sul (PROPESQ-UFRGS).

7. Author Contributions

P. O. Brum was responsible for project design and conducting experiments, data analysis and interpretation and manuscript and figure confection. G. D. Viola conducted experiments, data analysis and interpretation. C. Saibro-Girardi and C. Tiefensee-Ribeiro and J. Gasparotto provided technical support. M. O. Brum

reviewed the manuscript and provided help with statistical analysis. J.C.F. Moreira provided material support. R. Krolow reviewed the manuscript and figures. D. P. Gelain conceived the project, interpreted data, provided technical and material support, and reviewed the manuscript.

8. Conflict of Interests

The authors declare no conflict of interest.

9. References

1. Whittle, S. B., Smith, V., Doherty, E., Sibo, Z., McCarty, S., Zage, P. E., *Overview and recent advances in the treatment of neuroblastoma*, Expert Review of Anticancer Therapy, vol. 17(4), 2017, doi: 10.1080/14737140.2017.1285230
2. Huertas-Castaño, C., Gómez-Muñoz, M. A., Pardal, R., Vega, F. M., *Hypoxia in the Initiation and Progression of Neuroblastoma Tumours*, International Journal of Molecular Sciences, vol. 21(1), 2020, doi: 10.3390/ijms21010039
3. Smith, M. A., Seibel, N. L., Altekruse, S. F., Ries, L. A. G., Melbert, D. L., O'Leary, M., Smith, F. O., Reaman, G. H., *Outcomes for Children and Adolescents With Cancer: Challenges for the Twenty-First Century*, Journal of Clinical Oncology, vol. 28(15), 2010, doi: 10.1200/JCO.2009.27.0421.
4. Mohlin, S., Wigerup, C., Jögi, A., Pahlman, S., *Hypoxia, Pseudohypoxia and Cellular Differentiation*, Experimental Cell Research, 192-196, 2017, doi: 10.1016/j.yexcr.2017.03.007

5. Cimmino, F., Pezone, L., Avitabile, M.. Acierno, G., Andolfo, I., Capasso, M., Iolascon, A., *Inhibition of hypoxia inducible factors combined with all-trans retinoic acid treatment enhances glial transdifferentiation of neuroblastoma cells*, Scientific Reports, vol. 5, 2015, doi: 10.1038/srep11158
6. Lee, J., Bae, S., Jeong, J., Kim, S., Kim, K., *Hypoxia-inducible factor (HIF-1)α: its protein stability and biological functions*, Experimental & Molecular Medicine, vol. 36 (1), 2004, doi: 10.1038/emm.2004.1
7. Iommarini, L., Porcelli, A. M., Gasparre, G., Kurelac, I., *Non-Canonical Mechanisms Regulating Hypoxia-Inducible Factor 1 Alpha in Cancer*, Frontiers in Oncology, vol. 7, 2017, doi: 10.3389/fonc.2017.00286
8. Lim, J., Kim, H., Bang, Y., Seol, W., Choi, H. S., Choi, H. J., *Hypoxia-inducible factor-1α upregulates tyrosine hydroxylase and dopamine transporter by nuclear receptor ERRγ in SH-SY5Y cells*, NeuroReport, vol.16 (6), 2015, doi: 10.1097/WNR.0000000000000356
9. Ceci, C., Barbaccia, M. L., Pistritto, G., *A not cytotoxic nickel concentration alters the expression of neuronal differentiation markers in NT2 cells,* NeuroToxicology, vol. 47, 2015, doi: 10.1016/j.neuro.2015.01.001
10. Zhang, J., Song, L., Huang, Y., Zhao, Q., Zhao, K., Chen, G., *Accumulation of hypoxia-inducible factor-1α protein and its role in the differentiation of myeloid leukemic cells induced by all-trans retinoic acid*, Haematologica, vol. 93 (10), 2008, 10.3324/haematol.13096
11. Mishra, S., Kelly, K. K., Rumian, N. L., Siegenthaler, J. A., *Retinoic Acid Is Required for Neural Stem and Progenitor Cell Proliferation in the*

Adult Hippocampus, Stem Cell Reports, vol. 10, 2018, doi: 10.1016/j.stemcr.2018.04.024

12. Lee, J., Bae, S., Jeong, J., Kim, S., Kim, K., *Hypoxia-inducible factor (HIF-1)α: its protein stability and biological functions*, Experimental & Molecular Medicine, vol. 36 (1), 2004, doi: 10.1038/emm.2004.1
13. Esfahani, M., Karimi, F., Afshar, S., Niknazar, S., Sohrabi, S., Najafi, R., *Prolyl hydroxylase inhibitors act as agents to enhance the efficiency of cell therapy,* Expert Opinion on Biological Therapy, vol. 15 (12), 2015, doi: 10.1517/14712598.2015.1084281
14. Bhaskara, V. K., Mohanam, I., Rao, J. S., Mohanam, S.,*Intermittent Hypoxia Regulates Stem-like Characteristics and Differentiation of Neuroblastoma Cells*, PLoS One, vol. 7 (2), 2012, doi: 10.1371/journal.pone.0030905
15. Kovalevich, J., Langford, D., *Considerations for the Use of SH-SY5Y Neuroblastoma Cells in Neurobiology*, Methods in Molecular Biology, vol. 1078, 2013, doi: 10.1007/978-1-62703-640-5_2
16. Shipley, M. M., Mangold, C. A., Szpara, M. L., *Differentiation of the SH-SY5Y Human Neuroblastoma Cell Line*, Journal of Visualized Experiments, vol. 108, 2016, doi: 10.3791/53193
17. Filograna, R., Civiero, L., Ferrari, V., Codolo, G., Greggio, E., Bubacco, L., Beltramini, M., Bisaglia, M., *Analysis of the Catecholaminergic Phenotype in Human SH-SY5Y and BE(2)-M17 Neuroblastoma Cell Lines upon Differentiation*, PLoS ONE, vol. 10 (8), 2015, doi: 10.1371/journal.pone.0136769

18. Encinas, M., Iglesias, M., Liu, Y., Wang, H., Ceña, V., Gallego, C., Comella, J. X. *Sequential Treatment of SH-SY5Y Cells with Retinoic Acid and Brain-Derived Neurotrophic Factor Gives Rise to Fully Differentiated, Neurotrophic Factor-Dependent, Human Neuron-Like Cells*, Journal of Neurochemistry, vol. 75, 2000, doi: 10.1046/j.1471-4159.2000.0750991.x.
19. Studer, L., Csete, M., Lee, S., Kabbani, N., Walikonis, J., Wold, B., McKay R., *Enhanced Proliferation, Survival, and Dopaminergic Differentiation of CNS Precursors in Lowered Oxygen*, The Journal of Neuroscience, vol. 20 (19), 2000, doi: 10.1523/JNEUROSCI.20-19-07377.2000
20. Wang, Y., Jian Y., Haisheng L., Xuan W. , Lingling Z. , Ming F. *, Xiaomin W., *Hypoxia Promotes Dopaminergic Differentiation of Mesenchymal Stem Cells and Shows Benefits for Transplantation in a Rat Model of Parkinson's Disease*, PLoS One, vol. 8 (1), 2013, 10.1371/journal.pone.0054296
21. Pacary, E., Tixier, E., Coulet, F., Roussel, S., Petit, E., Bernaudin, M.,*Crosstalk between HIF-1 and ROCK pathways in neuronal differentiation of mesenchymal stem cells, neurospheres and in PC12 neurite outgrowth*, Molecular and Cellular Neuroscience, vol. 35 (3), 2007, doi: 10.1016/j.mcn.2007.04.002
22. Miyake, S., Muramatsu, R., Hamaguchi, M., Yamashita, T.,*Prolyl hydroxylase regulates axonal rewiring and motor recovery after traumatic brain injury*, Cell Death Discovery, vol. 6, doi: 10.1038/cddis.2015.5

23. Hämmerle, B., Yañez, Y., Palanca, S., Cañete, A., Burks, D. J., Castel, V., Font de Mora, J.,*Targeting Neuroblastoma Stem Cells with Retinoic Acid and Proteasome Inhibitor*, PLoS One, vol. 8 (10), 2013, doi: 10.1371/journal.pone.0076761
24. Coughlan, D., Gianferante, M., Lynch, C. F., Stevens, J. L., Harlan, L. C., *Treatment and survival of childhood neuroblastoma: Evidence from a population-based study in the United States*, Pediatric Hematology and Oncology, vol. 34 (5), 2017, doi:10.1080/08880018.2017.1373315
25. Jing, X., Yang, F., Shao, C., Wei, K., Xie, M., Shen, H., Shu, Y., *Role of hypoxia in cancer therapy by regulating the tumor microenvironment*, Molecular Cancer, vol. 18 (1), 2019, doi: 10.1186/s12943-019-1089-9
26. Petrova, V., Annicchiarico-Petruzzelli, M., Melino, G., Amelio, I., *The hypoxic tumour microenvironment,* Oncogenesis, vol. 7(10), 2018, doi: doi.org/10.1038/s41389-017-0011-9
27. Marxsen, J. H. , Stengel, P., Doege, K., Heikkinen, P., Jokilehto, T., Wagner, T., Jelkmann, W., Jaakkola, P., Metzen, E., *Hypoxia-inducible factor-1 (HIF-1) promotes its degradation by induction of HIF-α-prolyl-4-hydroxylases*, Journal of Biochemistry, 2004, doi: 10.1042/BJ20040620
28. Moroz, E., Carlin, S., Dyomina, K., Burke, S., Thaler H. T., Blasberg, R., Serganova, I., *Real-Time Imaging of HIF-1a Stabilization and Degradation*, PLOS One, vol. 4 (4), 2009, doi: 10.1371/journal.pone.0005077
29. Girardi, C. S., Rostirolla, D. C., Lini, F. J. M., Brum, P. O., Delgado, J., Tiefensee-Ribeiro, C., Teixeira, A. A., Peixoto, D. O., Heimfarth, L.,

Kunzler, A., Moreira, J. C. F., Gelain, D. P., *Nuclear RXRα and RXRβ receptors exert distinct and opposite effects on RA-mediated neuroblastoma differentiation,* Biochimica et Biophysica Acta (BBA) - Molecular Cell Research, vol. 1866 (3), 2019, doi: 10.1016/j.bbamcr.2018.11.014

30. de Ramos, V. M., Zanotto-Filho, A., de Bittencourt Pasquali, M.A., Klafke, K., Gasparotto, J., Dunkley , P., Gelain, D. P., Moreira, J. C. F., *NRF2 Mediates Neuroblastoma Proliferation and Resistance to Retinoic Acid Cytotoxicity in a Model of In Vitro Neuronal Differentiation*, Molecular Neurobiology, vol. 53 (9), 2016, doi: 10.1007/s12035-015-9506-6
31. Matthay, K. K., Maris, J. M., Schleiermacher, G., Nakagawara, A., Mackall, C. L., Diller, L.,Weiss, W. A., *Neuroblastoma*, Nature Reviews Disease Primers, vol 2, 2016, doi: 10.1038/nrdp.2016.78
32. Selak, M. A., Armour, S. M., MacKenzie, E. D., Boulahbel, H., Watson, D. G., Mansfield, K. D., Pan, Y., Simon, M. C., Thompson, C. B., Gottlieb, E., *Succinate links TCA cycle dysfunction to oncogenesis by inhibiting HIF-alpha prolyl hydroxylase*, Cancer Cell, vol. 7 (1), 2005, doi: 10.1016/j.ccr.2004.11.022
33. Koivunen, P., Hirsilä, M., Remes, A. M., Hassinen, I. E., Kivirikko, K. I., Myllyharju, J., *Inhibition of Hypoxia-inducible Factor (HIF) Hydroxylases by Citric Acid Cycle Intermediates*, Journal of Biological Chemistry, vol. 282 (7), 2007, doi: 10.1074/jbc.M610415200
34. de Bittencourt Pasquali, M. A., de Ramos, V. M., Albanus, R. D. *et al.* Gene Expression Profile of NF-κB, Nrf2, Glycolytic, and p53 Pathways

During the SH-SY5Y Neuronal Differentiation Mediated by Retinoic Acid, Molecular Neurobiology vol. 53, 2016, 10.1007/s12035-014-8998-9

35. Hong-Sheng Li, Yan-Ni Zhou, Lu Li, Sheng-Fu Li, Dan Long, Xue-Lu Chen, Jia-Bi Zhang, Li Feng, You-Ping Li, *HIF-1α protects against oxidative stress by directly targeting mitochondria*, Redox Biology, vol. 25, 2019, doi: doi: 10.1016/j.redox.2019.101109
36. Kunzler, A., Zeidán-Chuliá, F., Gasparotto, J., et al. *Changes in Cell Cycle and Up-Regulation of Neuronal Markers During SH-SY5Y Neurodifferentiation by Retinoic Acid are Mediated by Reactive Species Production and Oxidative Stress*, Molecular Neurobiology, 2017, vol. 54(9), doi: 10.1007/s12035-016-0189-4